ABSTRACT

Commonly in a structural air frame there are critical locations which have to be designed by keeping stress concentration factor in mind. Usually wings in the air frame are the lift load carrying members. Aerodynamic loads received by the body of the aero planes and ribs get transferred to spars based on the machining capability the spars can be designed in to two or more parts and later it can be assembled.

In an air planes weight design planes an important role in the aircraft design and development without compromising on the safety of the structure. Structure of the airframe represents one of the finest examples in minimizing aircraft design using strength of material approach.

The current project work includes the design & analysis of the spar beam using typical loads distributed on the beam. Design is to be carried out by considering the beam in to two parts.

In the present case small size transport aircraft structure is considered. Riveted joint used to fix and linear static analysis is employed to carry out analysis of spar beam. FEM approach is carried out for determining bending stresses and moments. In the analysis of aircrafts, Miner's rule is used for estimating the fatigue damage of critical components.

CHAPTER: 1

INTRODUCTION

In the last decades, the assessment of the service durability of aerospace components and assemblies has become an important segment of design, mostly because of the growing needs for the light-weight structures which will be safe and reliable, and at the same time, not too expensive. It is especially true for the main structural elements such as wing spar, fuselage bulkheads and fittings, whose sudden failure could lead to the catastrophic consequences. In order to meet the strict safety requirements, as well as to check structural components before usage, a number of expensive and long experiments are carried out. Taking into account ever-present manufacturers´ tendencies to shorten time-to-market periods, the use of finite element method (FEM) for the estimation of fatigue life has been proved as a good alternative to the experimental method [1].

The main function of the wings in aircraft is to provide lift. The wings have been classified as two essential parts, the internal wing structure consists of spars, ribs, stringers, and the external wing structure consists of skin.

Spar is a heavy beam in which different transverse shear load and shear bending is acting on the spar beam. It usually consists of thin panel (web) with a cap or flange at the top and bottom. Ribs are also used in the span wise distribution.

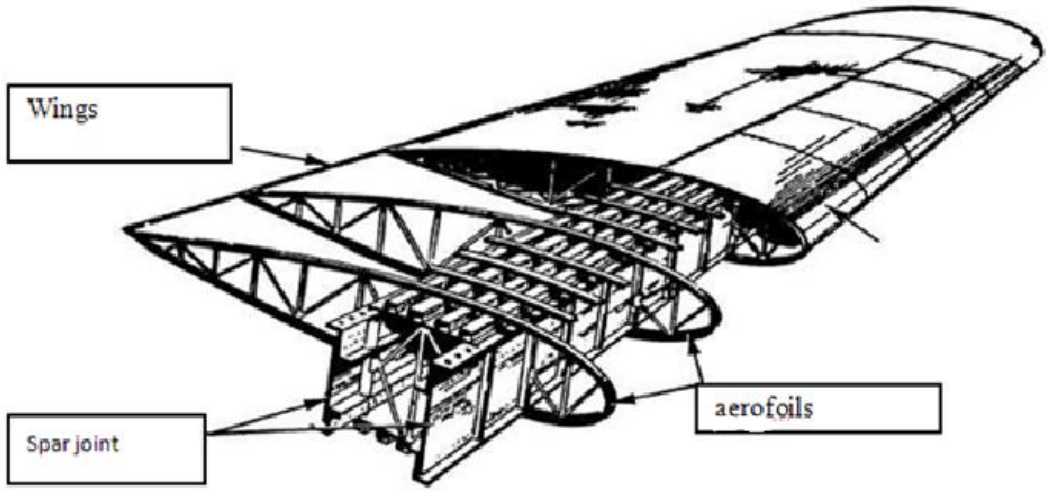

Figure 1.0 Schematic diagram of two wing spar joint

The work undertaken at present incorporates the outline and investigation of the flight part utilizing the variable loads located on the spar. Normally, in aircraft the outline is done by dividing the spars into two sections.

The linear static investigation is completed on the spar flange, and the examination is done on this joint so as to decide the greatest stress. The investigation is done by utilizing the FEM packages. AL2024-T351 material is used in this analysis. It is found that the maximum stress is induced are within allowable limits.

The phenomenon of weakening of the material due to the repeatedly applied alternative loads is called as fatigue. It may results in sudden failure [2].

Miners rule is used here to find out the total damage accumulation. Miner's rule states that if there are k different stress levels, number of accumulated cycles at i^{th} stress, Si is ni and the average number of cycle to failure at the i^{th} stress, According to this rule the failure of the structure will not occur when the damage fraction C is less than 1.

Additionally in the basic part the fatigue failure is generated due to high tensile stress acting on the critical region, a necessary fatigue calculation is carried out on the maximum stress.

The fatigue damage value is found within the critical damage, thus assuring the validity of a design.

1.1 Wing

Wing is constantly advanced from the starting 1930 to present 2016 i.e. BOEING etc. The difference between them is remarkable it depends on materials; number of lifting surfaces, size, and shape are used to provide the safe lifts to the aero planes. Since from 1930, NASA and its community NACA have been one of the co-founder for the wing design, developing the basic aerofoil shape and the airplanes manufacturers are used to provide the lift component for the shape air travel.

Basically there are 4 types of aircraft wing

a) Rectangular wing

b) Elliptical wing

c) Swept wing

d) Delta wing

a) Rectangular wing: It is likewise called Hershey bar, it is one sort of good reason wing it can convey sensible load and fly at rapid. It is utilized for the individual air ship and it can be control in high height, it is economical in construct and support.

Figure 1.1 Rectangular wing

b) Elliptical wing: It is similar to rectangular wing and it is utilized in tail wheel air craft since from 1930 up to 1940. Because of these large wings can catch the wind current effectively, giving airdrop without the help of forward momentum.

Figure 1.2 Elliptical wing

c) Swept wing: It is used in powerful jet aircraft and is need to forward momentum as compared to the rectangular wing and it can operate in high altitudes.

Figure 1.3 Swept wing

d) Delta wing: It advances the swept wing and it can be even pull further back in order to create drag due to this aircraft can fly in high altitude due to this it can be used in supersonic aircraft i.e. Figure fighter jets and also in spaceships.

Figure 1.4 Delta wing

1.2 Wing design

The main function of the wings of an aircraft is to provide lift. The wings considered as two essential parts. The internal wing structure consists of spars, ribs, stringers, and the external wing structure consists of skin.

The ribs also to be supported which is done by the spars. These are simple beams with different cross sections which is similar to an 'I' beam. A spar is considered as the majority of heavily load carrying component of an aircraft. In spars the majority of loads are carrying at its root, than at the tip. Due to wing will bend upwards, spars usually carries shear force and bending moment.

Commonly in wings due to aerodynamic forces not only bend the wing but also it twists. In order to avoid this introduce of second spar need to be essential. Commonly in modern aircraft often use two spars where the spars are joined by using

a torsion box structure, due to this torsion box serve as both spar caps (resist bending), and the torsion box (resist torsion) and to transmit the aerodynamic force.

1.3 Wing construction

a) Skin: external surface of the wing initially made up of fabric, cutting edge airplane utilizing aluminum because of light weight and rub safe properties.
b) Ribs and outsiders: they are made up of inter skeleton of wing, giving unbending nature and quality, adaptability is required of the flying machine, which were utilized as a part of flying in view of adaptability is important to retains stress during hard landing and turbulence.
c) Spar: it is utilized as a part of primary/focus light emission wing. It is utilized to transmit substantial burden were it is joined to the fuselage or body of the air ship.
d) Fuel tank: is joined generally in the wing and it is housed in an own tank and it is permitted to fill the holes between the ribs.
e) Flaps: they are high lift and high drag gadget they are utilized for a reason of lifting capacity at slower speed by changing the chamber or ebb and flow. It is additionally used to make drag.
f) Root: The wings root is one of the parts of a wing. It is connected to the fuselage or body of the flying machine.
g) Wing tip: it is utilized as a part of wing for the purpose of route light is mounted.
h) Stats: they are high lift device found on cleared or delta wing flying machine; they are mounted on the fundamental edge of the wing it can be used as a lifting limit.

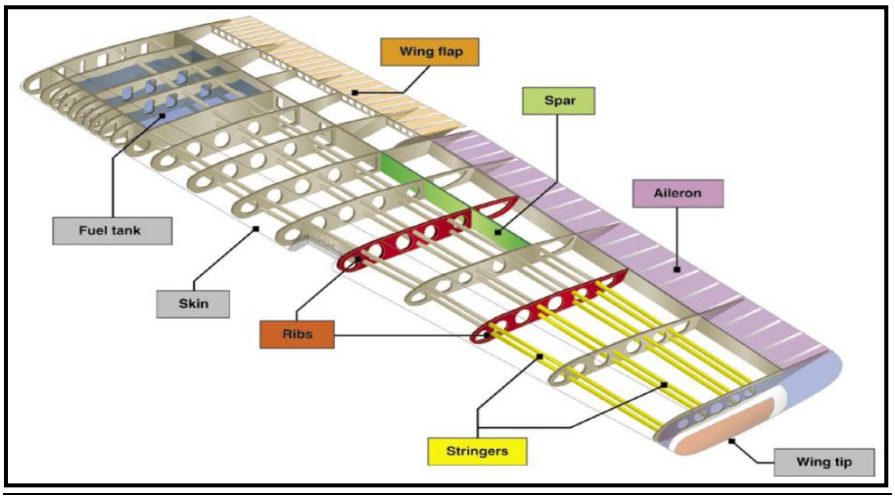

Figure 1.5 Basic construction of wing

1.4 Location of spars in web design

In earlier decades wings were designed with 3 or more spars, because to provide a reduction in rib stress and to provide a better supports. But now a day's aerospace industries were prefer two spars because of necessary space provided for the attachment of the fuel tank and landing gears.

Commonly two spar wing construction consists of front and rear spar, usually front spar is located such that leading edge slats are connected at the tip of the forward spar. For the rear spars is located such that control surfaces like stringers, flaps were used to connect it.

Hence forth front and rear spar are combined with wing skin panel forms a closing member of torsion box and also serves as a fuel tank.

1.5 Spar design

a) Cross section of spars

Cross section of spars consists of only two types

1. I section
2. C section

b) Types of spars

There are two types of spars

1. Shear web spar(commonly adopted in design of the modern wing)
2. Truss type

In an aircraft, spar is considered as one of the major component in the wing. Usually spar is used as a lifting capacity of the aircraft. Majority of the weight is acting on the spar usually spar is attached to the ring and one end of the spar is connected to the fuselage and other end is act as a free edge, so an obtained spar is a cantilever beam.

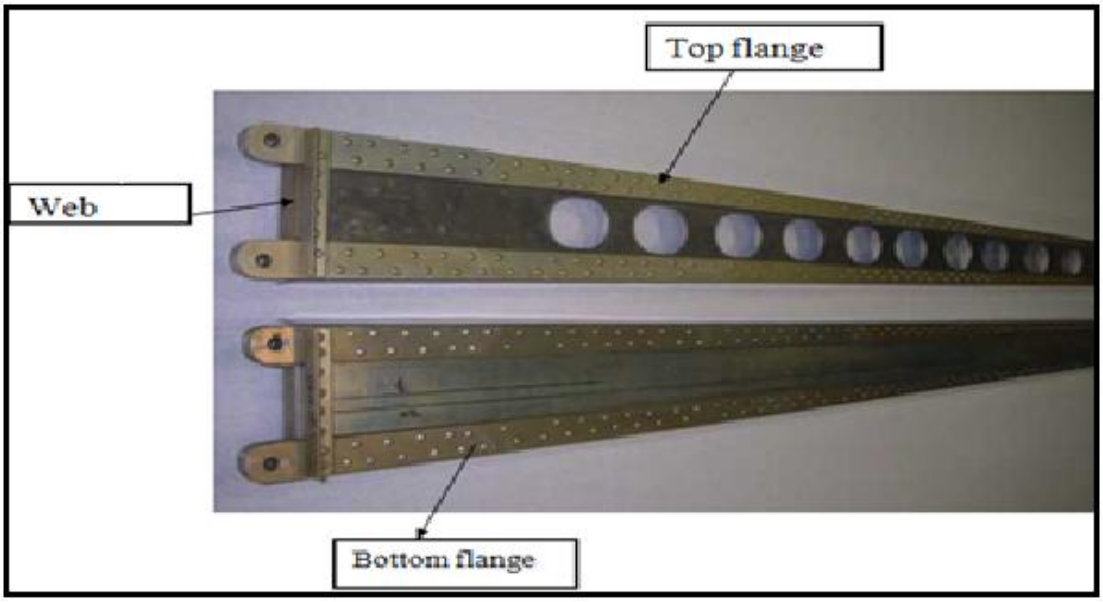

Figure 1.6 Spar design

1.6 Spar selection

We know that the spars are the major load carrying member in the wing with regarding to bending. From the bending moment it is likewise used to calculate greatest bending moment at the root and it is additionally used to compute the area of the spars and stingers.

1.7 Wing skin

Often the skin on a wing is plotted to support the part of the aircraft on the flight and the ground loads. Fuel is often carried inside the wings of a stressed skin. Aircraft fuel box is commonly attached to the wings of the aircraft and enough sealed is used to store the fuel in the aircraft and is also called wing design. And also it can be used in a transport category aircraft and reduces weight.

1.8 Aircraft materials

Basic aircraft materials are aluminum, titanium, steel combinations in the previous day's utilizations of cutting edge fiber composites, generally propelled composites materials have been situated in air ship up to half of air ship weight with respect to determination of materials. The following specification has been viewed as like cost, weight, structural performance, material cost, maintenance cost, fabricating cost.

Commonly used materials in aircraft industries are

1. Aluminum alloys
2. Titanium alloys
3. Steel alloys

Now from past decades, an application of advanced fiber composites has been rapidly increased till now. Some new commercial jets such as the BOEING 787 already contain composite material up to 50% of the aircraft weight. Many materials are available for the structural engineers, some of the most materials are commonly used in aerospace industries are listed below.

1. Aluminum alloys
2. Titanium alloys
3. Steel alloys
4. Composite material

1. Aluminum alloys

It is one of the commonly used materials in the aircraft structure, especially the 2024 and the 7074 alloys.

- It is one of the good material property packages
- It having a good fatigue characteristic
- It also having high yield strength
- It can be deformed into different shapes
- It having low melting temperature

2. Titanium alloys

Additionally to the aluminum alloys for the long time operation at maximum temperature about 150degC material than steel.

- It can elongate and stronger material than aluminum
- This can be used in industries up to 1000degC
- It is one of the best structural materials
- It is more expensive
- Machining capacity is low

3. Steel alloys

Steel alloys are made up of iron and carbons, with other constituents are also added. Because of alloys the strength can be increased, and it can be withstand at high temperature.

Eg – stainless steel, tool etc.

Regarding key performance of the air ship considers like thickness (weight), stiffness (young's modulus), strength (ultimate yield quality), sturdiness, harm resilience, consumption. Commonly in aircraft industries they will prefer aluminum 2024 has standard material in view of excellent fracture and slow toughness.

As compared to aluminum AL 7075 alloys, AL 2024 T351 has low break durability. It is used in fuselage and low wings skins. Recently developed AL-LI alloys offered enhanced properties over traditional compounds. They are around 10% stiffer and 10% lighter and have most elevated weakness performance.

Two sorts of materials have been considered in flying machines namely alloys and composites. In this metal will be utilized as a part of low load zones where huge measure of materials are required, for example, ribs, fuselage, skin, outlines, bulkheads and so forth.

1.9 Composite materials

In 1940 aircraft began to design synthetic material in order to enhance advanced design, since those times the composites have been used more and more not only in the fiber glass, graphite industry, but also in the aviation industry also for sports, auto racing, boating etc.

Commonly composites structure has defined as combination or mixture of different materials or things. Even in those combined state they are identified individually and separated with the help of mechanically stressed state.

1.10 Advantages and disadvantages of Aircraft materials

- Higher corrosion resistance
- Low cost
- Easily repairable
- Longer life of the metals

1.11 Disadvantages

- More hazardous to the environment
- Very expensive processing equipment
- It offered high toxic and more hazardous
- Lack of standard accuracy required for the construction and repairs

1.12 Primary material selection criteria

- Fatigue strength
- Availability and cost
- Fracture toughness and crack growth
- Corrosion and brittleness properties.

1.13 Aerofoil selection

It is having one type of symmetrical shape, it is used to produce high lift, high directional control during flight, it produces an aerodynamic force through the fluid.

A. Symmetrical Airfoils

Symmetrical airfoils have identical upper and lower surfaces. They are used to rotary-wing applications because they have no center of pressure. Travel remains stationary under varying angles of attack, it is having the best lift drag ratios for the full range of velocities from rotor blade root to tip. However, the symmetrical airfoil produces less lift than a nonsymmetrical airfoil and also has relatively undesirable stall characteristics.

Advantage of a Symmetrical Airfoil

- It can produce an equal amount of lift in either direction at the same positive or negative angle of attack.
- Negative lift can also be obtained with a cambered airfoil. (This means you can fly a cambered airfoil inverted).
- The inverted angle must be great enough, that the effective lower area of the airfoils (which is now, in reality the upper).

B. Cambered Airfoils

Nonsymmetrical (cambered) airfoils designed have a wide variety of upper and lower surface designs. The advantages of the nonsymmetrical airfoil are having a

high lift-drag ratios and more desirable characteristics. Non-symmetrical airfoils were not used in earlier helicopters because the center of pressure location was increased as we moved towards when angle of attack was changed. Cambered airfoils (asymmetric) are the airfoils which can generate a lift at a zero angle of attack.

1.14 Aerofoil nomenclature

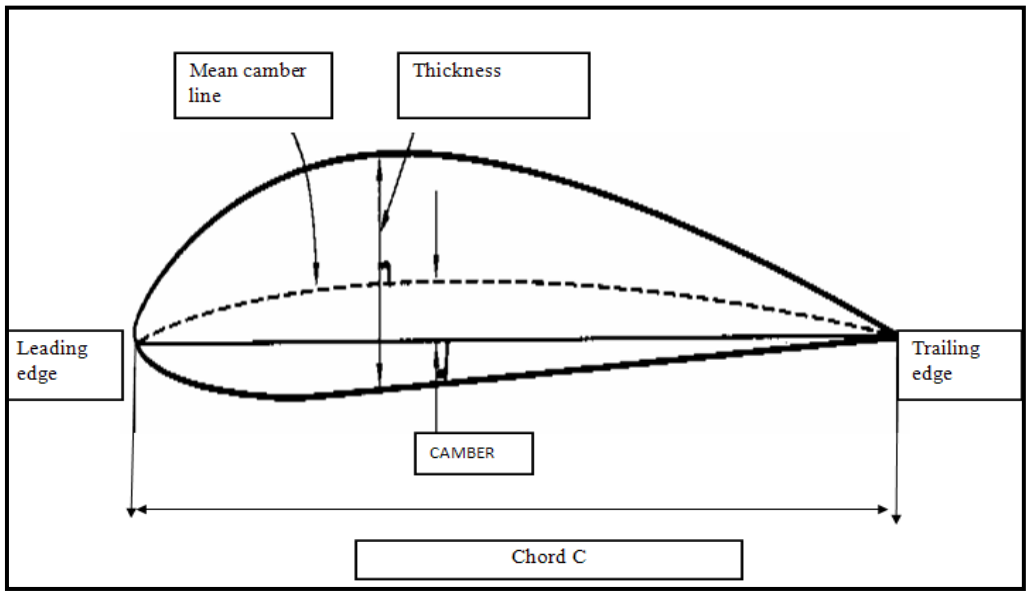

Figure 1.7 Aerofoil nomenclature

1. Chord(C) - distance between leading edge to tip edge which is acting parallel to the axis of symmetry.
2. Camber - larger distance between the mean camber line and the chord line.
3. Thickness – distance between upper and lower surface which is acting perpendicular to the axis of symmetry.

1.15 NACA (National Advisory Committee for Aeronautics)

1. It is fore- runner of NASA (National Aeronautics and Space Administration)
2. Methodically investigates the effects of various aerofoil parameters, due to the effects of aerodynamic behavior
3. Developed so many series of aerofoil and classification systems
4. Many of the aerofoil is still commonly used.
    - Four digits of series
    - Five digits of series
    - Six digits of series

1.15.1 Brief description about NACA aero foils

- First number is percentage of chord.
- Second number is maximum distance from the center, is measured from the leading edge.
- Last two digits give maximum thickness in percentage of chord.
- Designed with maximum lift coefficients is acting at the leading edge.
- The following series is acts for the laminar flow.

Figure 3.5 and Figure 3.6 clearly describe the two types of aerofoil's sections which are attached to the tip and root.

1. NACA 23014

- Max thickness 12% at 29.85% chord
- Max camber 1.8% at 12.7% chord

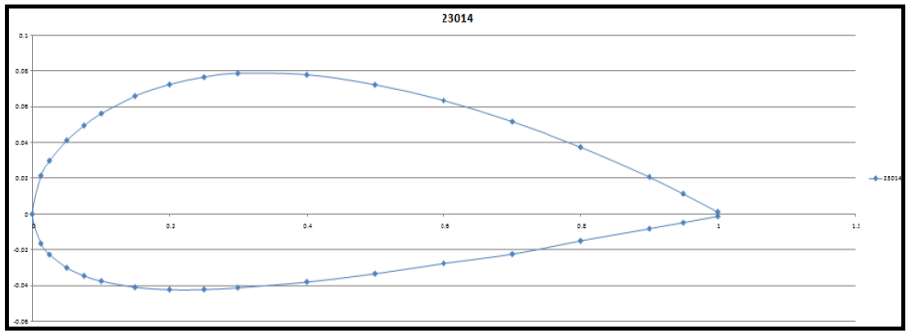

Figure 1.8 NACA 23014 aerofoil

2. NACA 23012

- Max thickness 14% at 30% chord
- Max camber 1.8% at 15% chord

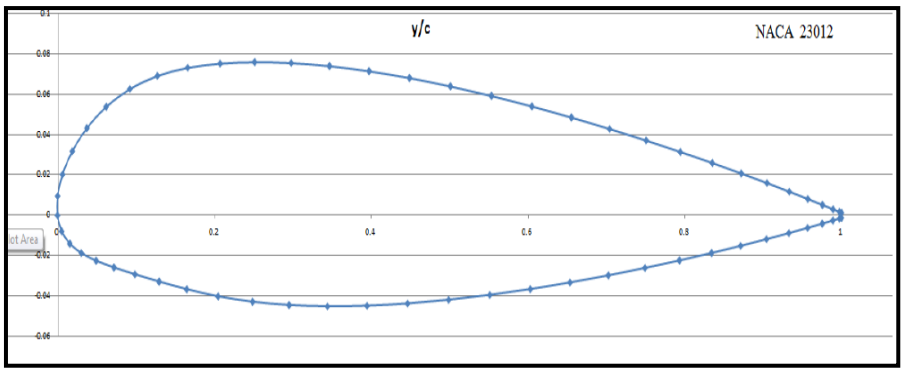

Figure 1.9 NACA 23012 aerofoil

CHAPTER: 2

LITERATURE SURVEY

Aleksandar Grbovic and Bosko Rasuo [1] carried out the tests on leading structural components like wing, spar etc, due to sudden load applied which lead to a catastrophic failure. In order to reduce this problem a necessary safety requirement has to be carried out and also have to check the structural components before usage. A series of experiments were carried out on the structural component, and the following process is too much expensive. In order to reduce this problem facing the best method used in industries to predict the fatigue life estimation is finite element method approach. Due to finite element approach, it is also possible to prevent the catastrophic failure obtained from the variable amplitude loading.

Nagarjun C M, Nagaraj V C, Byrareddy and K E Girish, **[2]** conducted a research on one of the critical component in aircraft. The analysis of stress is carried out by using horizontal tail. In order to examine the static and fatigue load carrying capacity, the acquired fatigue life estimation is done by using miner principle and the S-N bend is plotted by using the material aluminum 2024 T-6.

Rhys Jones, Daren Peng, Pu Huang, Raman R. K. Singh, **[3]** discussed the problem associated with crack growth on naturally occurring discontinuities in operational aircraft. The present study clearly illustrates that there is a little crack growth enclosure from its initial equivalent pre size (EPS) to final failure, and its can be easily and accurately computed.

R.M. Ajaj, M.I. Friswell , M. Bourchak , W. Harasani, **[4]** investigates about the range transforming idea for the apparatus driven self-sufficient twin fight (GNAT Fight) for a smaller than usual UAV. By utilizing this system the traverse augmentations can be accomplished up to 100% however for this condition. It can be lessened by up to 20% due to keeping in mind the end goal to expand drag and the high coefficient of lift. At last confinement and disadvantages of configuration is outlined and investigated.

Harish E.R.M, Mahesha.K, Sartaj Patel, **[5]** investigated on stress analysis of the wing attachment bracket, from this stress analysis it has found that the

maximum stress is found at one point of the rivet hole, due to obtained maximum stress the fatigue analysis has been carried out.

Raffaele Sepe, Enrico Armentani and Francesco caputo, **[6]** depicted the test on a full scale board with variable burden condition and the testing of model is completed on a triaxial testing machine. The analysis was performed by using different material by which the panel is composed. From this research it clearly shows that the numerical data clearly correlates with experimental data, and it successfully predicts the failure on the fuselage panel.

Polagnagu James, Kotresh Gaddikeri, Byji Varughese and M. Subba Rao, **[7]** presented about the shear flows around rectangular cross-section were unsymmetrical about both the axis, when subjected to biaxial bending and also torque is presented. An approximate procedure used for transforming shear flow from the aerofoil's of the wing structure to the wing box; the following experiment is carried out by using hydraulic jacks. The design ultimate load withstand successfully, without any defects was identified on the spar spliced plates.

Mohamed Hamdan A1, Nithiyakalyani S, **[8]** made investigation on the analysis of a ribs and spar of the commercial jet aircraft due to variable loads, the methodology of finite element method and detailed procedure of FEM tools has been utilized.

2.1 Outcome of the review

The entire process of the static analysis of spar joint of the finite element method has proved successful and reliable because calculated values matched the results of the experiment. Of course, it must not be forgotten that fatigue has stochastic nature and that the same spar under the same loading may show different fatigue behavior, i.e. the crack may occur soon or later and on other locations too. However, numerical models presented in this article may still be used for new crack growth simulations and estimations of the residual life of the light aircraft spar under variable amplitude loading.

CHAPTER: 3

OBJECTIVES & METHODOLOGY

3.1.1 OBJECTIVES & SCOPE OF THE PRESENT WORK:

The objective of the present work is to design and Analysis of Wing spar Joint for a Transport Aircraft Structure.

The scope of the present work is to,

- Design and analyse wing spar joint for a transport aircraft structure using 1D analysis.
- Design and analyse wing spar joint for a transport aircraft structure using 2D analysis.
- Determine the maximum stress on the wing spar joint and to maintain within the yield criteria.
- Estimate the Fatigue life for safe design.

3.2 METHODOLOGY

The method used to solve the above objectives is finite element method (FEM) and the software used is MSC NASTRAN, PATRAN.

3.2.1 Introduction to FEM

Theoretical approaches can be used to solve simple engineering structures (bars, beams, plates, columns etc.) to determine deformations, strains, stresses etc. However, this approach cannot be used to solve problems associated with the completed engineering structures. To overcome this problem finite element method (FEM) is used. This method can be used to solve simple as well as completed engineering problems. This method can also be used to solve non-engineering problems. But the solutions obtained from FEM are approximate; hence it is essential to validate the solutions obtained from FEM either from experimental approaches or by using convergence criteria. FEA is the powerful tool to solve the simple and complicated problems. Finite element method is one of the numerical methods that can be used to solve the complicated partial differential and engineering equations. The basic idea behind finite element method is to find the solution for complex problem by dividing the problem into number of smaller segments and then each

individual segment can be analysed separately. At the end the solutions of all the segments can be algebraically added and then the solution of complicated structure can be obtained under its equilibrium conditions.

3.3 Generic Steps to Solve Problem using FEM

Generally the analysis is carried out by using the basic 3 types namely,

- Pre processing
- Solving
- Post processing

1 Pre processing:

- The geometry is to defined for the given problem
- Proper material properties is given to the problem
- Proper element connectivity is defined to the given problem(meshing)
- Proper load and boundary conditions is given to the problem

2 Solving:

- The obtained model is set to different analysis like linear static analysis, buckling analysis, thermal analysis.

3 Post processing:

- In post processing the obtained results from the solving is set to display in the form of plot or in the form of print.

3.4 SOFTWARE USED

3.4.1 MSC SOFTWARE:

- It is one of the general software used to carry out finite element analysis in aerospace industries.
- This type of software is commonly preferred in industries for the analysis is carried out for the critical geometry.
- Commonly in this software an obtained model is fine meshed and divided into each part called element, and this process is carried out is called discritization.
- Finally obtained results can be easily tabulated.

3.4.2 XFLR5 SOFTWARE

It is the analysis tool for airfoils, wings, and panel. It includes the x foil program for foil analysis and several 3-D analyses for the analysis of planes. An equation forms a structural network for standalone wings. The latest version V6 introduces stability analysis of planes.

3.4.3 PATRAN

PATRAN is one of the most pre/post processing technique for FEA using solid meshing technique and including post processing technique for various solver including MSC NASTRAN, ANSYS and PAMCRASH etc.

PATRAN provides a rich set of tools for the analysis of models including linear, non linear, dynamic thermal analysis in these cases meshes are created on surfaces using fully automated, meshing routines that provide combination of both finally load boundary conditions and analysis set up for the most popular solvers.

It is used in commonly aircraft industry for the meshing and analysis of prototype model and for twisting stress and breaking happens on the metal.

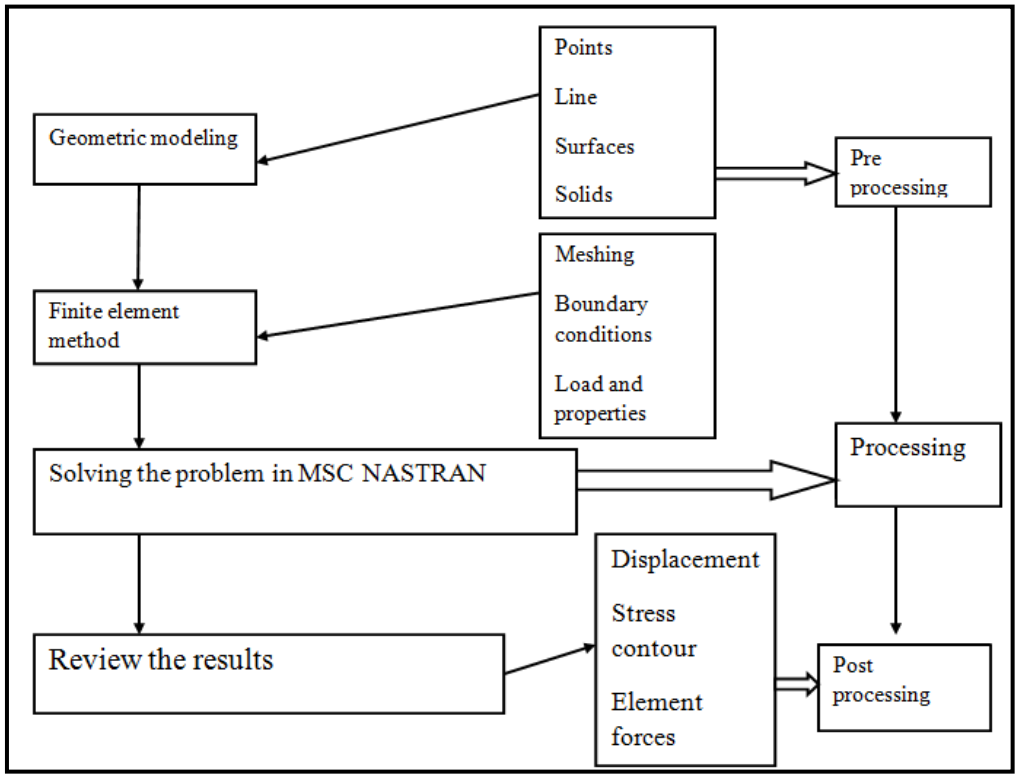

Figure 3.1 Basic flow chart of a NASTRAN run.

There are two numerical methods which is commonly used for the calculation of stress in aircraft components

3.5 Linear static analysis

Flow chart for static load analysis

- A 2-D modeling of spar beam is created by using PATRAN software.
- The analysis of spar beam is done by using MSC NASTRAN software.
- Match the obtained results with the theoretical, if it valid than the obtained design is safe.

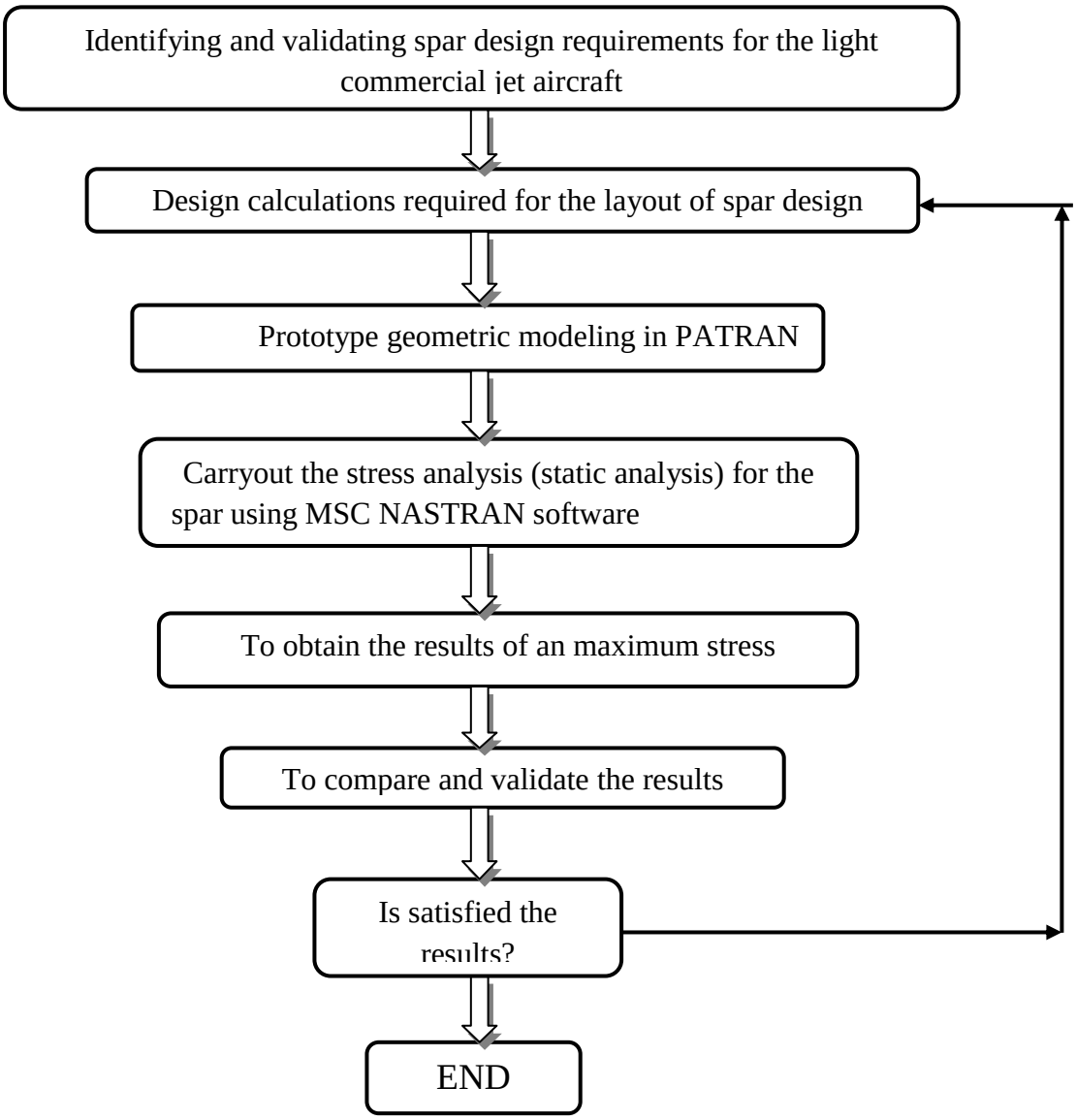

Figure 3.2 Flow chart of a static load analysis

In a direct static investigation the stress, strain, reaction forces under the effect of applied loads are calculated.

A series of assumptions are made with respect to a linear static analysis

- Less deflection.
- Small rotations
- Material properties
- Constant boundary conditions

Assumptions

- Deflections is nearly little with respect to the structure
- Rotation should be either 10 degree to 15 degree
- Material should be either linear elastic.
- Boundary conditions must be fixed.

3.6 Fatigue analysis

Commonly in aircraft about majority of component caused failure is either due to fatigue. Experimentally proved that more than 95% caused is either due to fatigue, due to this damage some of them are unrecoverable it is either due to following reasons.

1. It is either due to change in a material behavior, because of this fatigue has been generated and also effects in changes of material behavior.
2. It is also due to when material is rest and also when the fatigue stress is removed. Because of this commonly unrecoverable material behavior can be seen.

Regularly in eighteenth century fatigue failures can be seen normally in railroad axles. It is either because of repeated cyclic loading the fracture has been generated. Also the obtained fracture is due to the stress amplitude is within the elastic range of the material.

When subjected to a huge number of cycles at stress levels when subjected to monotonic yield strength, a portion of the Wohler information are plotted for Krupp hub steel regarding nominal stress(S) v/s number of cycles to failure (F), the obtained plot to be known as S-N bend. Every bend is still described to as Wohler line.

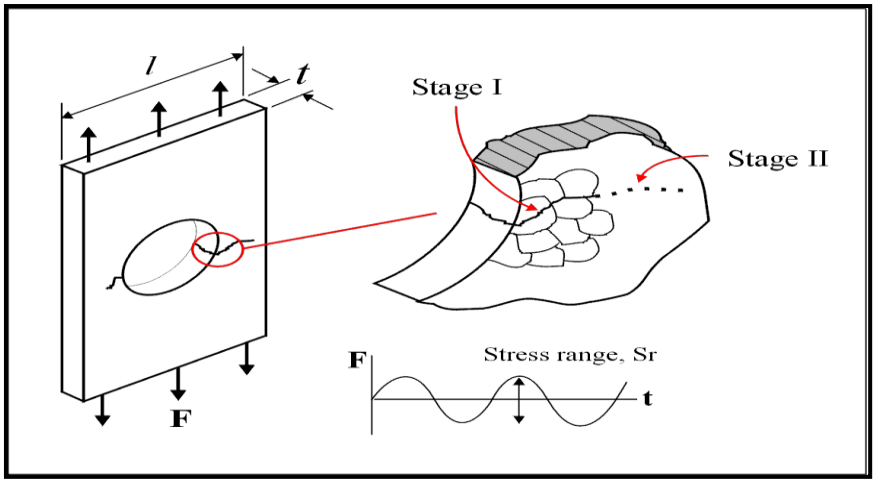

Figure 3.2 Crack initiations at the (1) and (2) stages

The following diagram determines a straight forward segment subjected to a uniform sinusoidal variable force. After some time the crack get initiated at a critical region within the circumference of the hole. Due to this crack initiates after applying some induced stress on the components will be able to fail.

Commonly in this fracture the cracks can be generated in to two stages.

1. Crack initiation stage(first stage)
2. Crack growth stage(second stage)

- The influence on the loading type

When the loads are varied in the material from one region to another due to this endurance limit different loadings can be used namely.

Table 3.1 Influence of loading type

Measured loading	Target loading	C_{load}
Axial	Bending	1.25
Axial	Bending	0.725
Bending	Torsion	0.58
Bending	Axial	0.8
Torsion	Axial	1.38
Torsion	Bending	1.72

CHAPTER 4

FINITE ELEMENT MODEL DEVELOPMENT

1 MODEL 1: 1D wing spar joint of a transport aircraft structure for static analysis.

2 MODEL 2: 2D wing spar joint of a transport aircraft structure for static analysis.

3 MODEL 3: Determine the maximum stress on the wing spar joint and to maintain within the yield criteria.

4.1 MODEL 1: 1D wing spar joint of a transport aircraft structure for static analysis.

The geometric model of aircraft wing spar was designed by using MSC NASTRAN software as shown in the bellow figure 4.1. The spar is a part of the aircraft in which different transverse shear load and shear bending is acting. It usually consists of thin panel (web) with a cap or flange at the top and bottom. Ribs are also used in the span wise distribution.

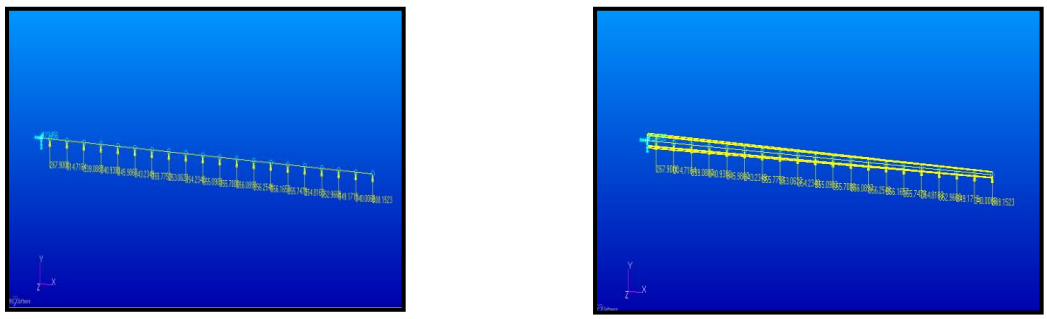

a) 1D line **b) 3D view of full span**

Figure 4.1 Geometric model for 1D analysis

For the static analysis to be performed first step is to construct the finite element model. The elements chosen for this is 21 nodes and 487.5 elements. Once the model has been constructed the next step is to define the material property, the material used is AL2024 T3. Mechanical properties of AL2024 T351 and Dimensions of the spar joint are shown in Table 4.1 and 4.2 respectively. The next step is to mesh the model; the size of the mesh depends upon the thickness of the spar. Once the

material property is assigned we are left with the boundary condition in the pre-processor stage. Properties like thickness, orientation, sections and material are assigned to the finite elements. The variable loads with different thickness acting on the spar joint as shown in figure 3.2(c). This completes the preprocessing work. The geometry of the model is shown in Fig 3.2(a). The Finite Element Model under boundary conditions is shown in Fig 3.2(b).

4.1.1 Material Specification

Aluminum alloys are widely used in modern aircraft construction. Aluminum alloys are valuable because they have high strength-to-weight ratio. Aluminum alloys are corrosion resistant andcomparatively easy to fabricate. The outstanding characteristic of aluminum is its lightweight. Selection of aircraft materials depends on the cost and its structural performance. The key material properties which are essential to maintain structural performance are:Density, Young's modulus, Ultimate and Yield strengths , Fatigue strength, Damage tolerance (fracture toughness and crack growth) and Corrosion, etc.

Table 4.1 Mechanical Properties of Aluminium 2024-T351

Property	**Aluminium**
Ultimate Tensile Strength	483 MPa
Tensile Yield Strength	362 MPa
Young's Modulus	70 GPa
Poisson's Ratio	0.33

Aluminium 2024-T351 is used for pressure bulkhead components and rivet. Table 4.1 describes material properties of Aluminium 2024-T351 used for the wing spar joint of a transport aircraft structure.

Table 4.2 Dimensions of 1D spar joint for Static analysis

Stations	Distance from root (mm)
0	0
1	125
2	375
3	625
4	875
5	1125
6	1375
7	1625
8	1875
9	2125
10	2375
11	2625
12	2875
13	3125
14	3375
15	3625
16	3875
17	4125
18	4375
19	4625
20	4875

4.1.3 Load and boundary conditions

Uniformly varying load was applied at tip side of the spar joint and other end is fixed which is called the root side of the spar joint. A two dimensional linear static stress analysis is carried out using finite element analysis software PATRAN and MSC NASTRAN. Mesh independent stress magnitudes are obtained through iterative mesh refinement process. Aluminum 2024-T351 alloy properties are given to the Pre-processor material properties. Load corresponding to the maximum lift load on the spar is considered. The different variable loads at each section are shown in figure

4.2. Along with dimensions used for variable load at each section along with different length are shown in table 4.4.

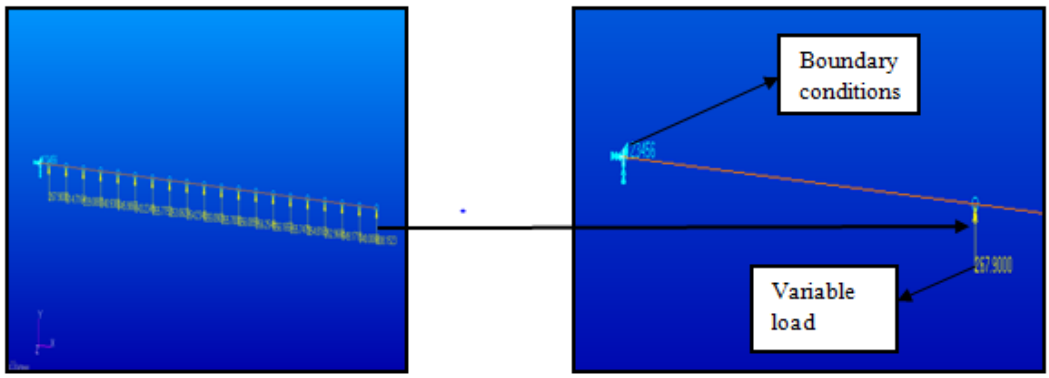

Figure 4.2: Load and boundary conditions of the 1D spar joint

Table 4.3 Dimensions of different varying load at each section for Static analysis

Stations	Distance from root (mm)	Loads on each section (kg)
0	0	0
1	125	267.98
2	375	314.7164
3	625	339.0887
4	875	340.9382
5	1125	345.98665
6	1375	344.23492
7	1625	345.7753
8	1875	354.0627
9	2125	354.23405
10	2375	355.0903
11	2625	355.69995
12	2875	356.089715
13	3125	356.2548
14	3375	356.16575
15	3625	355.7479
16	3875	354.8163

17	4125	352.9668
18	4375	349.1719
19	4625	340.0066
20	4875	308.1522731

4.2 MODEL 2: 2D wing spar joint of a transport aircraft structure for static analysis

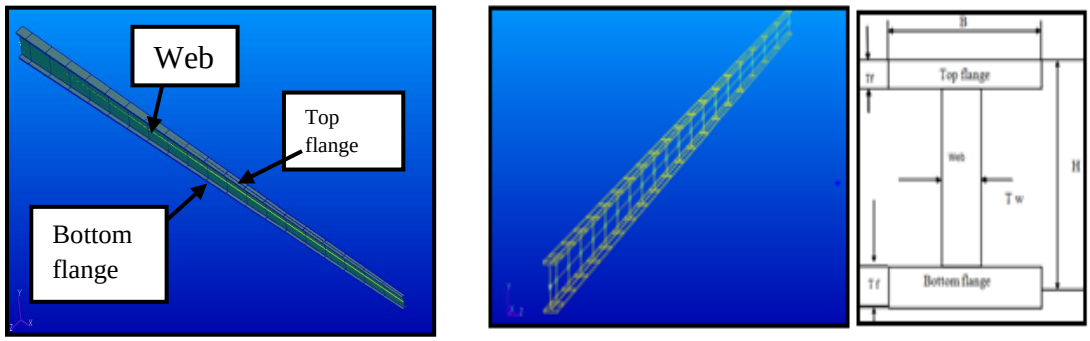

a) Geometry **b) I section view of spar joint**

Figure 4.3 Geometric model for 2D analysis

For the static analysis to be performed first step is to construct the finite element model. The elements chosen for this is 10455 nodes and 9949 elements. Once the model has been constructed the next step is to define the material property, the material used is AL2024 T3. Mechanical properties of AL2024 T351 and Dimensions of the spar joint are shown in Table 4.1 and 4.2 respectively. The next step is to mesh the model; the size of the mesh depends upon the thickness of the spar. Once the material property is assigned we are left with the boundary condition in the pre-processor stage. Properties like thickness, orientation, sections and material are assigned to the finite elements. The variable loads with different thickness acting on the spar joint as shown in figure 3.2(c). This completes the preprocessing work. The geometry of the model is shown in Fig 3.2(a). The Finite Element Model under boundary conditions is shown in Fig 3.2(b).

4.2.1 Material Specification

Aluminum alloys are widely used in modern aircraft construction. Aluminum alloys are valuable because they have high strength-to-weight ratio. Aluminum alloys are corrosion resistant andcomparatively easy to fabricate. The outstanding characteristic of aluminum is its lightweight. Selection of aircraft materials depends on the cost and its structural performance. The key material properties which are essential to maintain structural performance are:Density, Young's modulus, Ultimate and Yield strengths , Fatigue strength, Damage tolerance (fracture toughness and crack growth) and Corrosion, etc.

Table 4.4 Mechanical Properties of Aluminium 2024-T351

Property	**Aliminium**
Ultimate Tensile Strength	483 MPa
Tensile Yield Strength	362 MPa
Young's Modulus	70 GPa
Poisson's Ratio	0.33

Aluminium 2024-T351 is used for pressure bulkhead components and rivet. Table 4.1 describes material properties of Aluminium 2024-T351 used for the wing spar joint of a transport aircraft structure.

Table 4.5 Dimensions of 2D spar joint for Static analysis

station	t_w (mm)	t_f (mm)	B(mm)	D(mm)	b(mm)	d(mm)
0	6.65	5.9317	64.16	114.338	57.51	102.4746
1	6.225	5.545	64.256	112.713	57.031	101.621
2	5.90682	5.26185	61.4382	109.463	55.526	98.9393
3	5.58085	4.972	59.60885	106.213	54.028	96.269
4	5.2365	4.6653	57.7848	102.963	52.5483	94.6324
5	4.8789	4.3461	55.6909	99.713	51.182	91.1208
6	4.5089	4.0165	54.1369	99.463	49.628	88.430
7	4.1284	4.678	52.313	94.213	48.1846	85.857
8	4.7406	4.3323	50.489	89.963	46.7486	84.2985
9	4.3464	2.9814	48.665	86.713	45.3186	80.7502
10	2.9491	2.65716	46.84110	84.463	44.892	78.20868
11	2.5505	2.2724	45.017	80.213	42.4665	75.6682
12	2.1551	1.9205	44.193	76.963	41.1379	74.7232
13	1.76726	1.5745	41.36925	74.713	39.60194	70.564
14	1.53603	1.369	37.7212	67.213	37.7212	67.213
15	1.3267	0.85705	37.3564	66.563	37.3564	66.563
16	0.71424	0.63635	35.8973	64.963	35.8973	64.963
17	0.4304	0.384	34.073	60.713	34.073	60.713
18	0.1982	0.176905	32.249	57.463	32.249	57.463
19	0.049	0.04365	30.4254	547.213	30.4254	54.213
20	0	0	28.6014	50.963	28.6014	50.963

4.2.2 Finite Element Model

Quadrilateral element shown in Figure 4.5 are used to discretize the spar joint. Quadrilateral element has four nodes and each node has six degrees of freedom. Finite element model of the pressure bulkhead is having 10455 nodes and 9949 elements. Continuity is maintained between the elements and nodes to get accurate results. For every mesh component verification is necessary to correct the following factors in the meshed model and to check for the problem like duplicate element, unconnected nodes and duplicate boundaries, aspect ratio, warp angle, tapper and skew ratio are verified to check the quality in meshing.

A type of element used in this study are shown in the Figure 4.5.

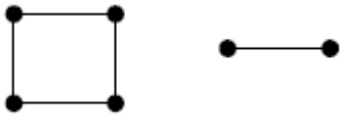

Figure 4.4: Four nodded quadrilateral element and 2 nodded bar element

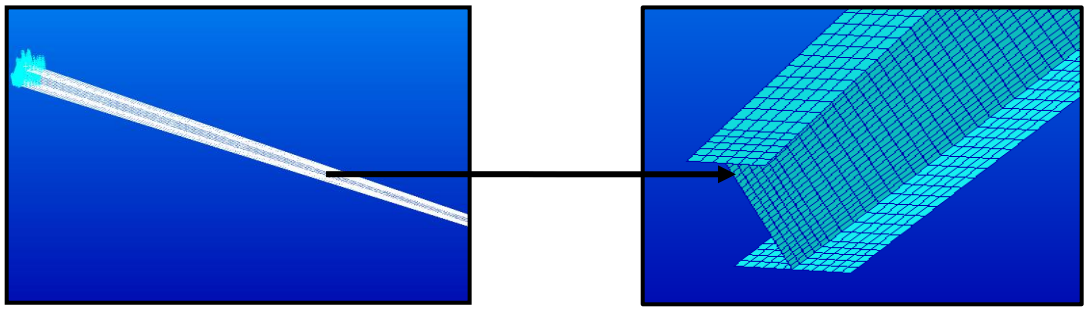

Figure 4.5: Finite element model of spar joint

Table 4.6 element and nodes used in spar joint

Parts of the spar joint	Type of element	Number of elements	Number of nodes	Aspect ratio
Top flange	Quadrilateral element	2928	2760	5
web	Quadrilateral element	4093	9000	5
Bottom flange	Quadrilateral element	2928	13669	5

4.2.3 Load and boundary conditions

Uniformly varying load was applied at tip side of the spar joint and other end is fixed which is called the root side of the spar joint. A two dimensional linear static stress analysis is carried out using finite element analysis software PATRAN and MSC NASTRAN. Mesh independent stress magnitudes are obtained through iterative mesh refinement process. Aluminum 2024-T351 alloy properties are given to the Pre-processor material properties. Load corresponding to the maximum lift load on the spar is considered. The different variable loads at each section are shown in figure 4.2. Along with dimensions used for variable load at each section along with different length are shown in table 4.4.

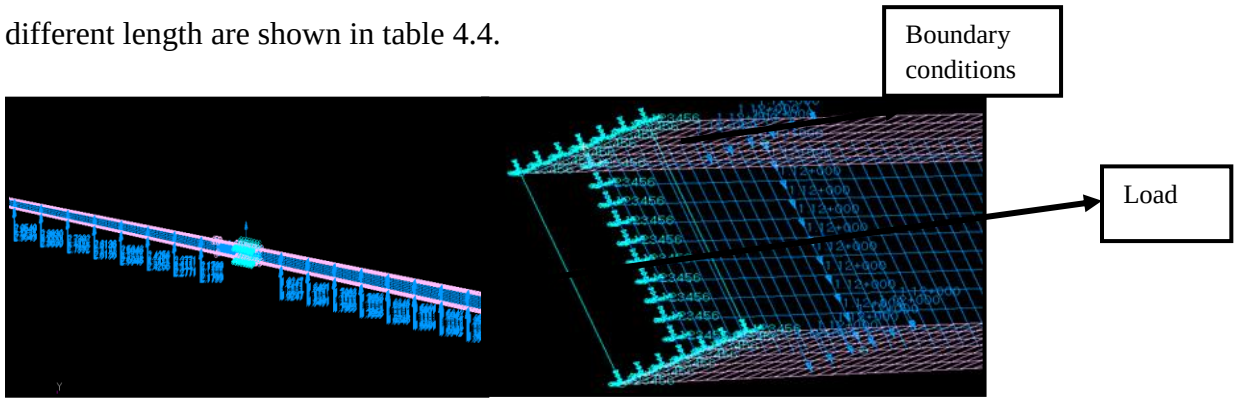

Figure 4.5: Load and boundary conditions of the spar joint

Table 4.7 Dimensions of different varying load at each section for Static analysis

Stations	**Distance from root (mm)**	**Loads on each section (kg)**
0	0	0
1	125	267.98
2	375	314.7164
3	625	339.0887
4	875	340.9382
5	1125	345.98665
6	1375	344.23492
7	1625	345.7753
8	1875	354.0627
9	2125	354.23405
10	2375	355.0903

11	2625	355.69995
12	2875	356.089715
13	3125	356.2548
14	3375	356.16575
15	3625	355.7479
16	3875	354.8163
17	4125	352.9668
18	4375	349.1719
19	4625	340.0066
20	4875	308.1522731

4.3 MODEL 3: Determine the maximum stress of the wing spar of the wing spar joint and to maintain the stress with in yield criteria.

The geometric configuration of the C clamp joint was designed by using MSC NASTRAN software has been shown in bellow figure 4.3. The C clamp joint are used to connect between two spar joint has been divided with the distance of length 2450mm and distance of length 2325mm. the devided sections has been showed in bellow figure 4.6.

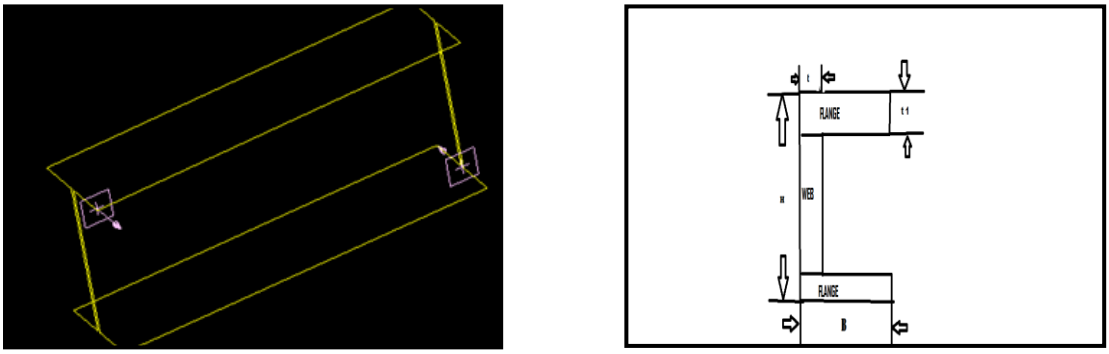

Figure 4.6 Geometric configuration of C clamp joint

In this case the static analysis follows the same procedure as explained in previous section. The constructed finite element model was divided into two sections of length 2450mm and length 2325mm. In order to connect between the two spars the C clamp joint was designed by using MSC NASTRAN software. The geometric configuration of a C clamp joint has been showed in figure 4.3. Once the model has

been constructed the next step is to define the material property, the material used is AL2024 T351. Mechanical properties of AL2024 T351 and Dimensions of the C clamp joint are shown in Table 4.1 and 4.2 respectively. The next step is to mesh the model; the size of the mesh depends upon the thickness of the spar. Once the material property is assigned we are left with the boundary condition in the pre-processor stage. The variable loads with different thickness acting on the spar joint as shown in figure 3.2(c). This completes the preprocessing work. The geometry of the model is shown in Figure 4.3. The Finite Element Model under boundary conditions is shown in Figure 4.6.

Table 4.8 Dimensions of C clamp joint for Static analysis

	Front C section (mm)	**End C section (mm)**	**Thickness (mm)**
Top flang	46.29392	46.29392	2.5
Bottom flang	46.29392	46.29392	2.5
Web	82.488	82.488	3

4.3.1 Finite element model

Quadrilateral element shown in Figure 4.5 are used to discretize the C clamp joint. Quadrilateral element has four nodes and each node has six degrees of freedom. Finite element model of the spar joint is having 10455 nodes and 9949 elements. Continuity is maintained between the elements and nodes to get accurate results. For every mesh component verification is necessary to correct the following factors in the meshed model and to check for the problem like duplicate element, unconnected nodes and duplicate boundaries, aspect ratio, warp angle, tapper and skew ratio are verified to check the quality in meshing.

A type of element used in this study are shown in the Figure 4.6.

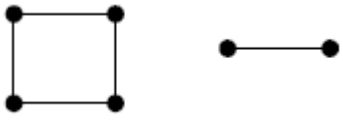

Figure 4.7: Four nodded quadrilateral element and 2 node

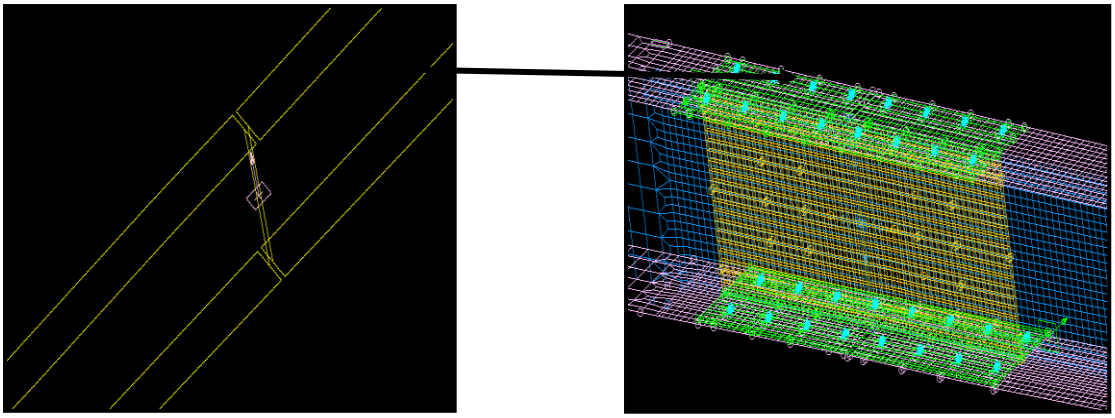

a) Divided spar **b) placing C clamp**

Figure 4.8: Finite element model of a 2D C clamp

The devided section must be 2mm a part and for this distance a joint is designed by designing proper rivets of thickness as shown bellow. The clamp attached to the spar of thickness 3mm in web and thickness 4.5mm in flanges at each section has been showed bellow. The rivets are the connecting elements which are used to connect the two divided spars. For a designed C clamp joint the following forces are acting on the parts of the C clamp joint, tensile forces(top flange, bottom flange), compressive forces(web) . Rivets are created by using 1D bar element. Rivits having circular cross-section with 2.5mm radius are used for this purpose. The rivets have been designed of 5/32 inches of 501kg load acting on each rivet. Finite element model of the rivet are shown in the Figure4.7(a). The finite element model of the pressure spar joint with rivet connections are shown in the Figure 4.7(b).

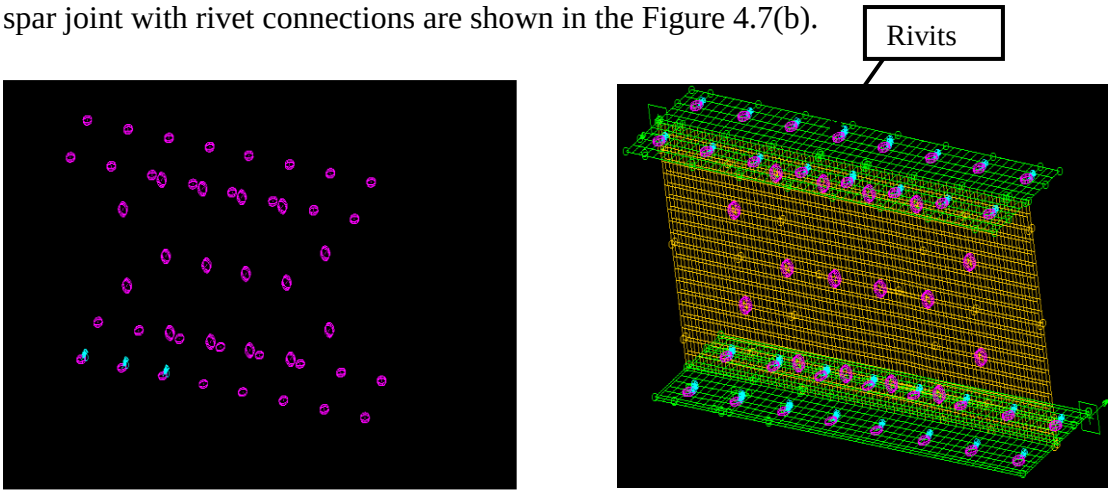

a) Rivets **b) C clamp riveted to spar.**

Figure 4.9: Finite element model of rivets

Table 4.9 Element and nodes used in C clamp joint

Parts of the spar joint	Type of element	Number of elements	Number of nodes	Aspect ratio
Top flange	Quadrilateral element	576	689	5
web	Quadrilateral element	1920	2068	5
Bottom flange	Quadrilateral element	480	3729	5
rivet	Bar	64	22	5

After placing the C clamp joint in between the spars. The directions are given to the rivet, in order to locate the rivet in particular direction i.e. along the Z direction. The directions are given to the rivet as showed in bellow figure.

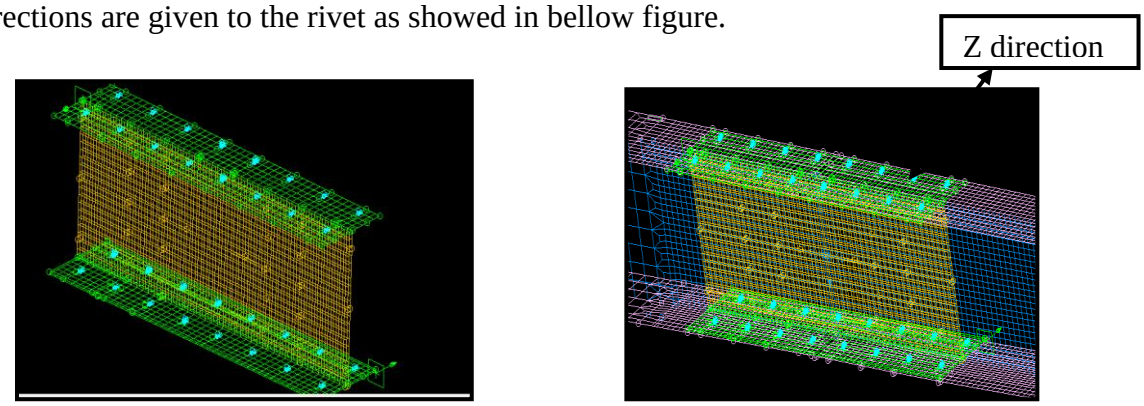

a) Riveted C clamp joint **b) placing between the spars**

Figure 4.10: The directions are given to the rivets

CHAPTER: 5

RESULTS AND DISCUSSIONS

Civil transport aircraft is used for carrying passengers from one place to another. Aircraft is a highly complex flying structure. Generally transport aircraft undergoes nominal maneuring flights. During the flight when the maximum lift is generated, the wings of the aircraft will undergo highest bending moment. The bending moment will be maximum at the root of the wing which caused highest stress at this location. Wings are attached to the fuselage structure through spar joint. The bending moment and shear loads from the wing are transferred to the fuselage through the attachment joints. In this project bending load transfer joint is considered for the analysis. First one needs to ensure the static load carrying capability of the spar joint. Stress analysis will be carried out for the given geometry of the spar joint. Finite element method is used for the stress analysis. In the current project, an attempt will be made to predict the fatigue life of spar joint in a transport airframe. In a metallic structure fatigue manifests itself in the form of a crack which propagates. Fatigue cracks will appear at the location of high tensile stress locations. These locations are invariably of high stress concentration. Fatigue life calculation will be carried out for typical service loading condition using constant amplitude S-N data for various stress ratios and local stress history at stress concentration.

5.1 Bending moment analysis of spar beam using 1D analysis

It is the vital step towards the design of the aircraft wing, Calculating SFD and BMD is one of the bases of analyzing beams and cantilever. Because of shear force diagram and bending moment diagram helps in design of every parameter namely spar etc. figure 4.1 shows the span wise load distribution the table 4.1 shows the span length and load distribution which helps in determining the maximum bending stress.

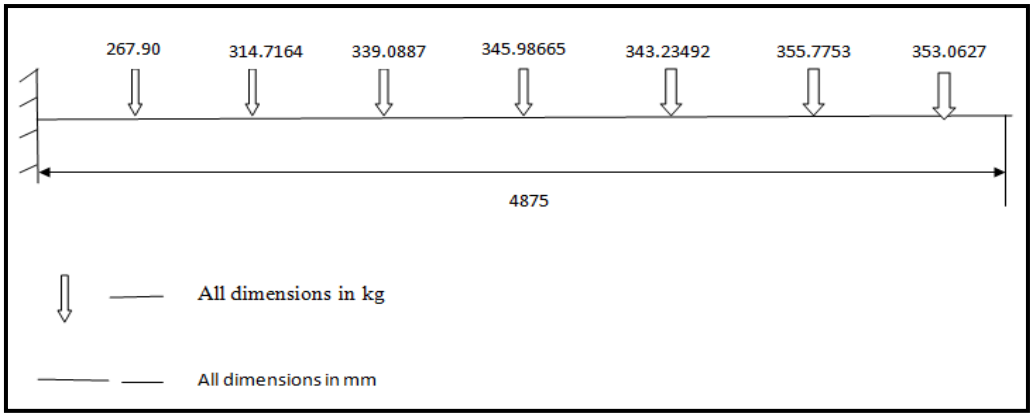

Figure 5.1 Span wise load distributions

Table 5.1 Span length and load distribution of spar joint

Stations	Distance from root (mm)	Loads on each section (kg)
0	0	0
1	125	267.98
2	375	314.7164
3	625	339.0887
4	875	340.9382
5	1125	345.98665
6	1375	344.23492
7	1625	345.7753
8	1875	354.0627
9	2125	354.23405
10	2375	355.0903
11	2625	355.69995
12	2875	356.089715
13	3125	356.2548
14	3375	356.16575
15	3625	355.7479
16	3875	354.8163
17	4125	352.9668
18	4375	349.1719
19	4625	340.0066
20	4875	308.1522731

The cantilever spar beam of varying cross section of span length (4875mm) and loads starting from (308.1522731 to 267.90kg) at different cross sections. Once the model has been constructed the next step is to define the material property, the material used is AL2024 T351. The material properties of aluminum AL2024 T351 are defined bellow.

Table 5.2 Mechanical Properties of Aluminium 2024-T351

Property	**Aliminium**
Ultimate Tensile Strength	483 MPa
Tensile Yield Strength	362 MPa
Young's Modulus	70 GPa
Poisson's Ratio	0.33

The following cantilever beam also indicates the different bending moment at different cross sections also the I sections values are tabulated in table 4.3
The bending stress values for each stations is calculated bellow

$$\sigma_b = \frac{\text{bending moment}}{BD^3 - bd^3/12} * Y_{max} \quad \ldots\ldots(4.1)$$

Table 5.3 I section tabulated values for the spar section

station	**Bending moment(N-m)**	**t_w (mm)**	**t_f (mm)**	**B(mm)**	**D(mm)**	**b(mm)**	**d(mm)**
0	17354867.98	6.65	5.9317	64.16	114.338	57.51	102.4746
1	15852625.65	6.225	5.545	64.256	112.713	57.031	101.621
2	14280095.12	5.90682	5.26185	61.4382	109.463	55.526	98.9393
3	12752468.06	5.58085	4.972	59.60885	106.213	54.028	96.269
4	11296480.01	5.2365	4.6653	57.7848	102.963	52.5483	94.6324
5	9921566.846	4.8789	4.3461	55.6909	99.713	51.182	91.1208

6	8631980.708	4.5089	4.0165	54.1369	99.463	49.628	88.430
7	7429921.302	4.1284	4.678	52.313	94.213	48.1846	85.857
8	6316625.052	4.7406	4.3323	50.489	89.963	46.7486	84.2985
9	5292867.121	4.3464	2.9814	48.665	86.713	45.3186	80.7502
10	4359154.753	2.9491	2.65716	46.84110	84.463	44.892	78.20868
11	3515815.29	2.5505	2.2724	45.017	80.213	42.4665	75.6682
12	2763067.934	2.1551	1.9205	44.193	76.963	41.1379	74.7232
13	2101075.371	1.76726	1.5745	41.36925	74.713	39.60194	70.564
14	1522940.509	1.53603	1.369	37.7212	67.213	37.7212	67.213
15	1050992.494	1.3267	0.85705	37.3564	66.563	37.3564	66.563
16	661757.5125	0.71424	0.63635	35.8973	64.963	35.8973	64.963
17	363436.5875	0.4304	0.384	34.073	60.713	34.073	60.713
18	1515016.15	0.1982	0.176905	32.249	57.463	32.249	57.463
19	33487.5	0.049	0.04365	30.4254	547.213	30.4254	54.213
20	0	0	0	28.6014	50.963	28.6014	50.963

From the table 4.3 we concluded that the analytical yield strength value of AL 2024 T351 material (350MPA), matches theoretical yield strength value. So the obtained design is safe. The plot of bending moment versus span length was shown in figure 4.2.

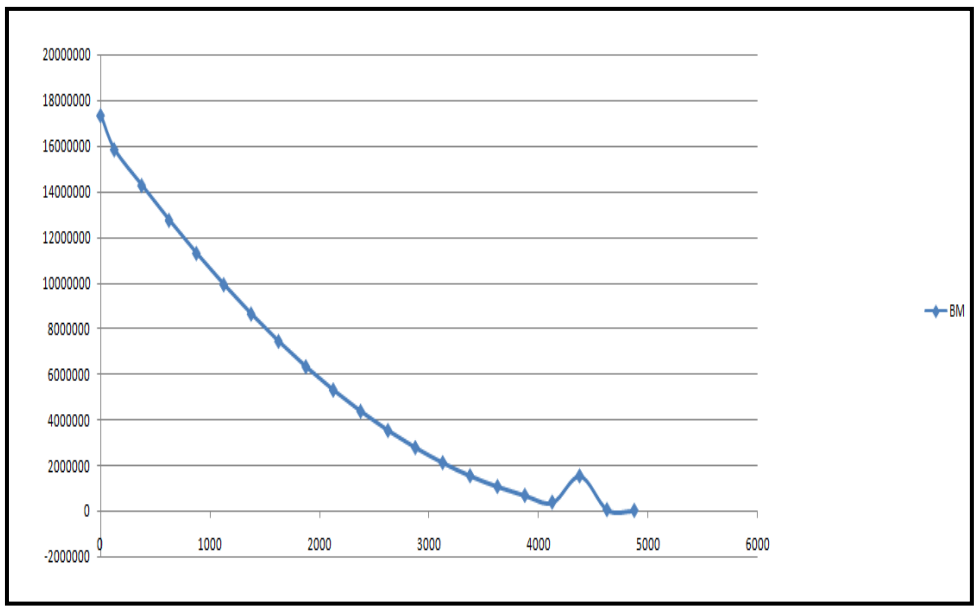

Figure 5.2 Plot of bending moment versus span length

After the completion of preprocessing work in 1D analysis the next step is to determine the maximum bending moment. The maximum bending moment analysis process is carried out by using MSC NASTRAN software. The figure 4.2 shows the maximum bending moment using 1D analysis.

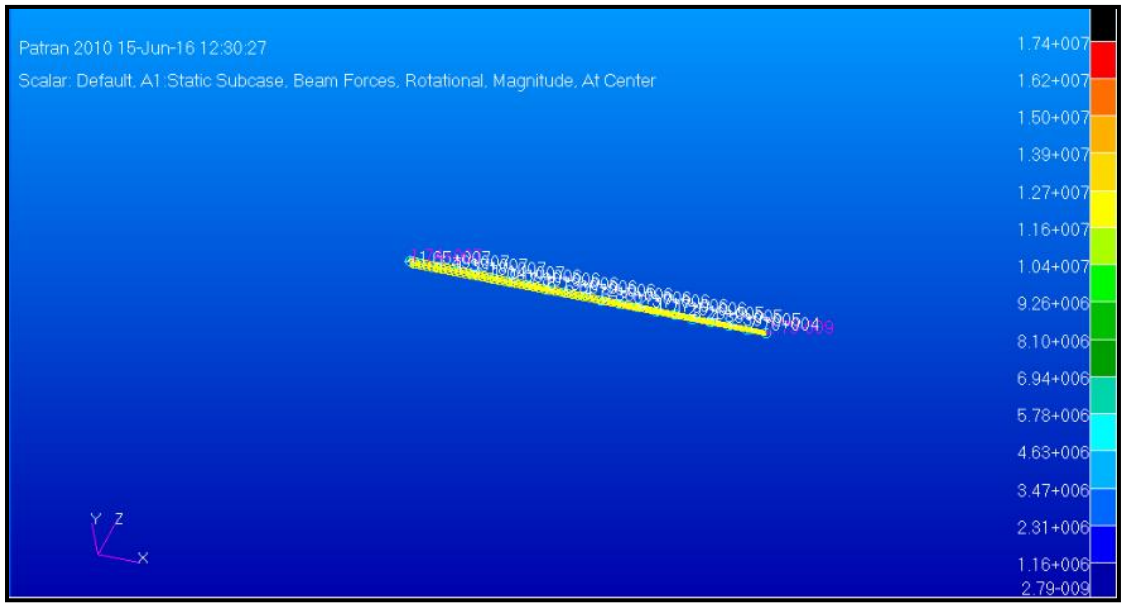

Figure 5.3 Maximum bending moment by using 1D analysis.

The maximum bending moment was found to be 1.74N-m. However theoretical value of bending moment was found to be 1.74N-m and it matches the theoretical value. Hence it considered to be safest design.

5.2 Static analysis of spar beam using 1-D

Now in NASTRAN the PATRAN file (bdf file) corresponding to model used in this analysis will be opened and then run option is selected thereby it takes few amount of solving time and gives the value of stresses. The important point to be noted here is that at the initial stage the structure was modeled in terms of inches and imported into PATRAN. The loads are applied in terms of kg. Since the model dimensions are in inch and the load applied is in kg the results will be in the form of kg and inch. The figure 4.3 shows the deformation of spar joint in 1D analysis.

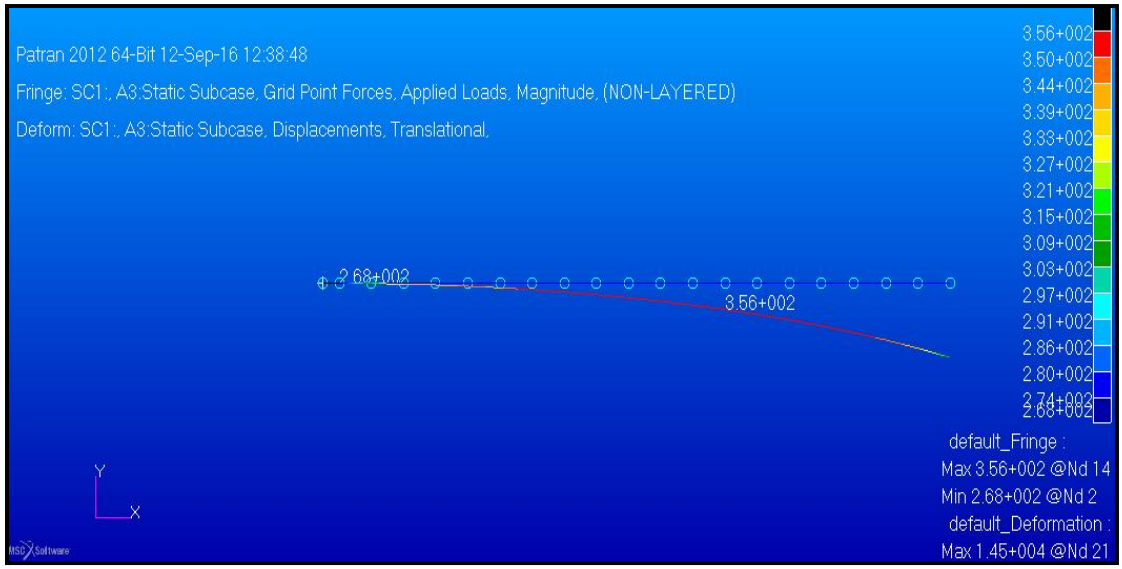

Figure 5.4 Deformation of spar joint by using1D analysis.

Figure 4.4 shows the static analysis of spar beam using 1-D. The static analysis is carried out by using analysis software (MSC software).

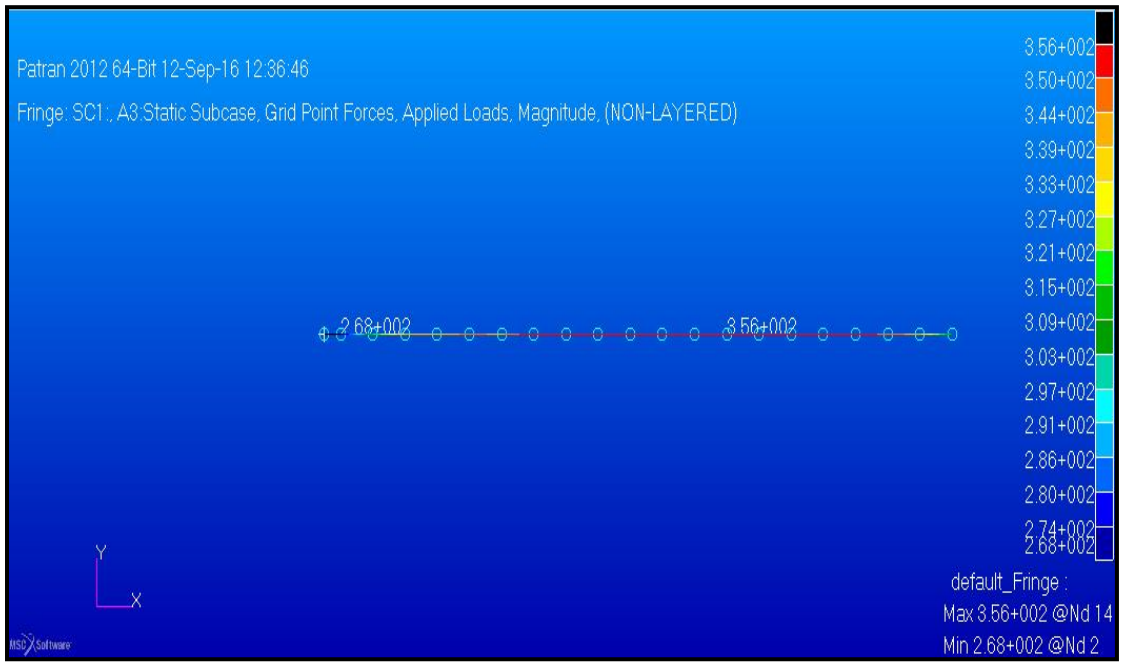

Figure 5.5 Static analyses of spar joint by using 1D in N/mm^2

The maximum stress is found to be 356 N/mm^2 . However, the tensile yield strenght of the aluminium 2024-T351 is 362 MPa. The induced stress level is found to be less than the allowable stress limit of the material used in the design of spar joint by using 1-D analysis. Hence, the static analysis of spar joint is considered to be safe design. Table 4.2 details the result summary of the static analysis of the spar joint using 1-D analysis.

Table 5.3 Result summary of the static analysis of the spar joint using 1-D analysis.

station	Stress (N/mm^2)
0-1	356
1-2	350
2-3	344
3-4	339
4-5	333
5-6	327
6-7	321
7-8	315
8-9	309
9-10	303
10-11	297
11-12	291
12-13	286
13-14	280
14-15	274
15-20	268

5.3 Static analysis of spar beam using 2-D

Now in NASTRAN the PATRAN file (bdf file) corresponding to model used in this analysis will be opened and then run option is selected thereby it takes few amount of solving time and gives the value of stresses. The important point to be noted here is that at the initial stage the structure was modeled in terms of inches and imported into PATRAN. The loads are applied in terms of kg. Since the model dimensions are in inch and the load applied is in kg the results will be in the form of kg and inch. The figure 4.3 shows the deformation of spar joint in 2D analysis.

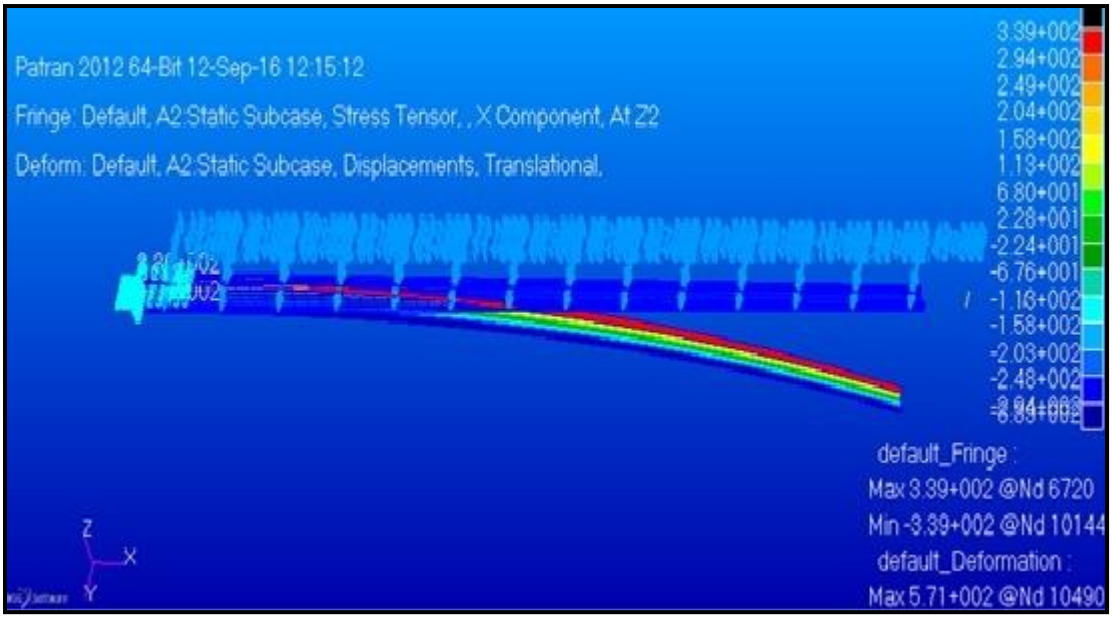

Figure 5.6 Deformation of spar beam by using 2D analysis

Figure 4.5 shows the static analysis of spar beam using 2-D. The static analysis is carried out by using analysis software (MSC software).

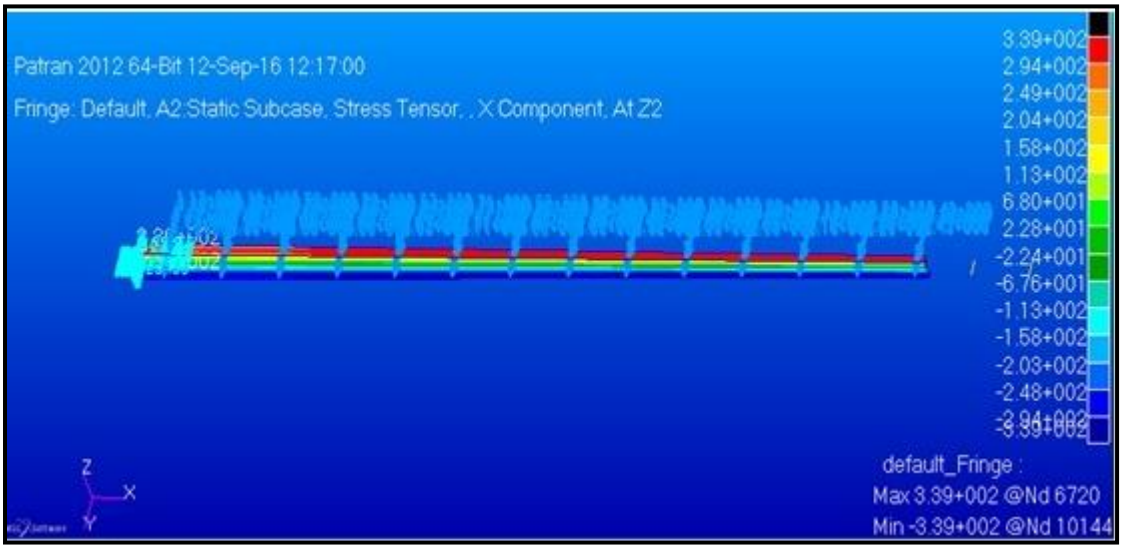

Figure 5.7 Static analysis of spar beam using 2-D

The maximum stress is found to be 339 N/mm^2 . However, the tensile yield strenght of the aluminium 2024-T351 is 362 MPa. The induced stress level is found to be less than the allowable stress limit of the material used in the design of spar joint by using 2-D analysis. Hence, the static analysis of spar joint is considered to be safe design. Table 4.3 details the result summary of the static analysis of the spar joint using 2-D analysis.

Table 5.4 Result summary of the static analysis of the spar joint using 2-D analysis.

station	stress(N/mm^2)
0-1	339
1-2	294
2-3	249
3-4	204
4-5	158
5-6	113
6-7	68
7-8	22.8
8-9	-22.4
9-10	-67.6
10-11	-113
11-12	-158
12-13	-203
13-14	-248
14-15	-294
15-16	-339

5.4 To determine the maximum stress of the spar beam using 2-D

Now in NASTRAN the PATRAN file (bdf file) corresponding to model used in this analysis will be opened and then run option is selected thereby it takes few amount of solving time and gives the value of stresses. The important point to be noted here is that at the initial stage the structure was modeled in terms of inches and imported into PATRAN. The loads are applied in terms of kg. Since the model dimensions are in inch and the load applied is in kg the results will be in the form of kg and inch. The figure 4.6 shows the deformation of 2-D spar joint using 2D analysis.

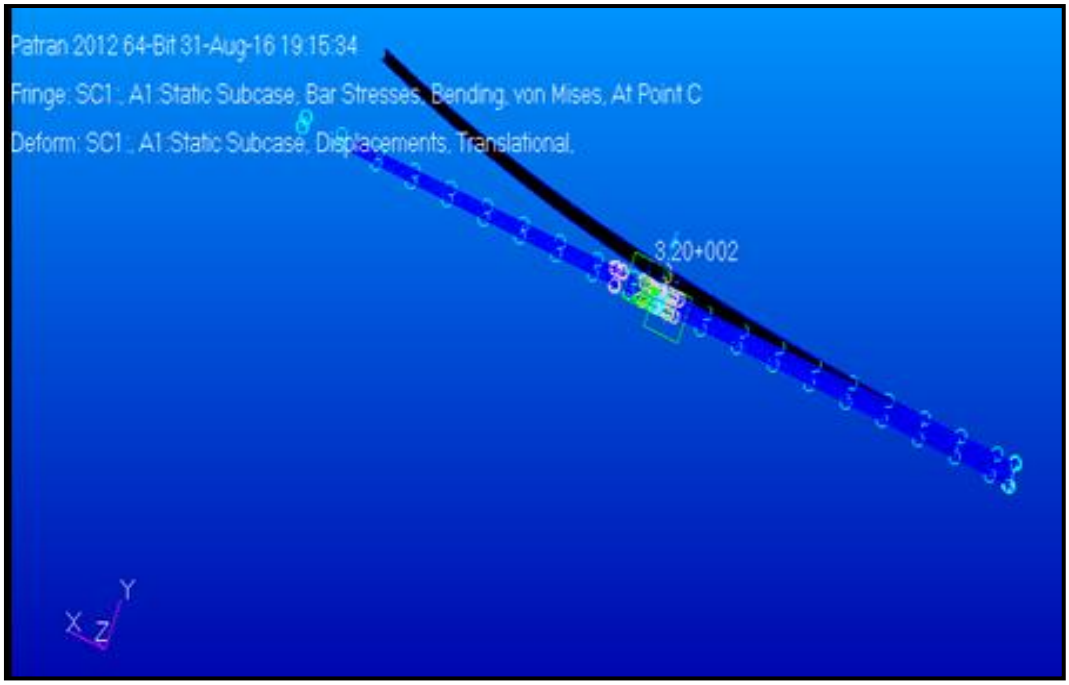

Figure 5.8 Deformation of 2-D spar joint using 2D analysis

Figure 4.7 shows the static analysis of spar joint using 2-D. The static analysis is carried out by using analysis software (MSC software).

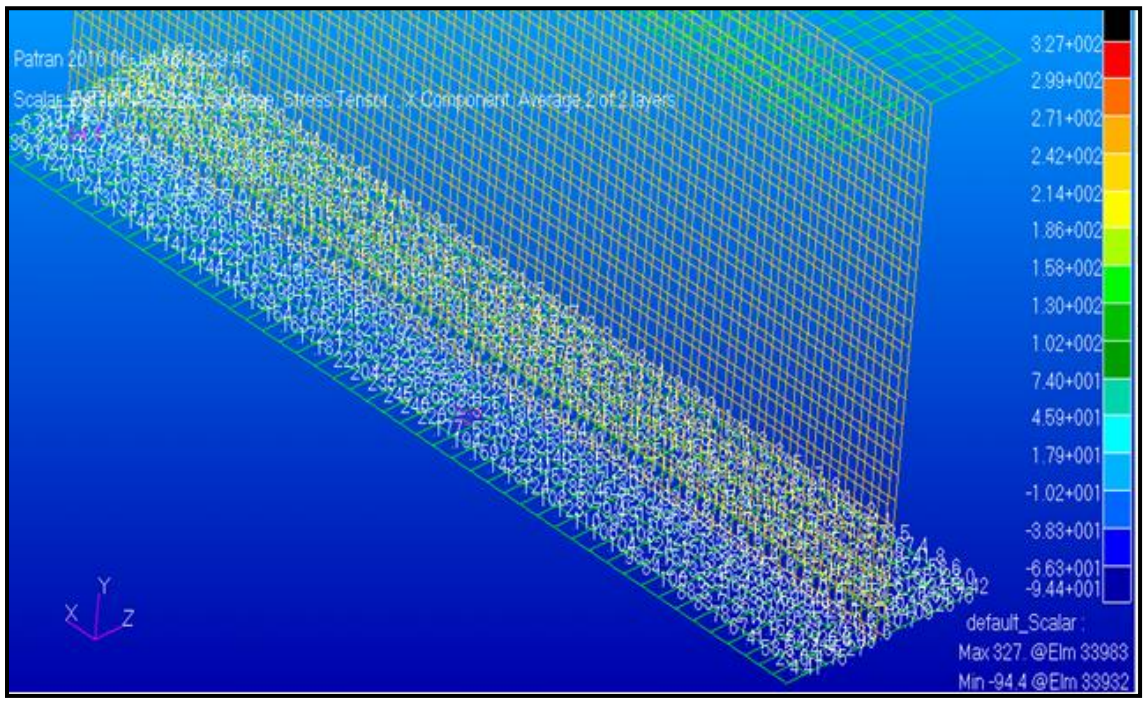

Figure 5.9 Static analysis of spar joint using 2-D

Figure 4.8 shows the maximum stress is obtained at 1 end of the rivet location. The static analysis is carried out by using analysis software (MSC software).

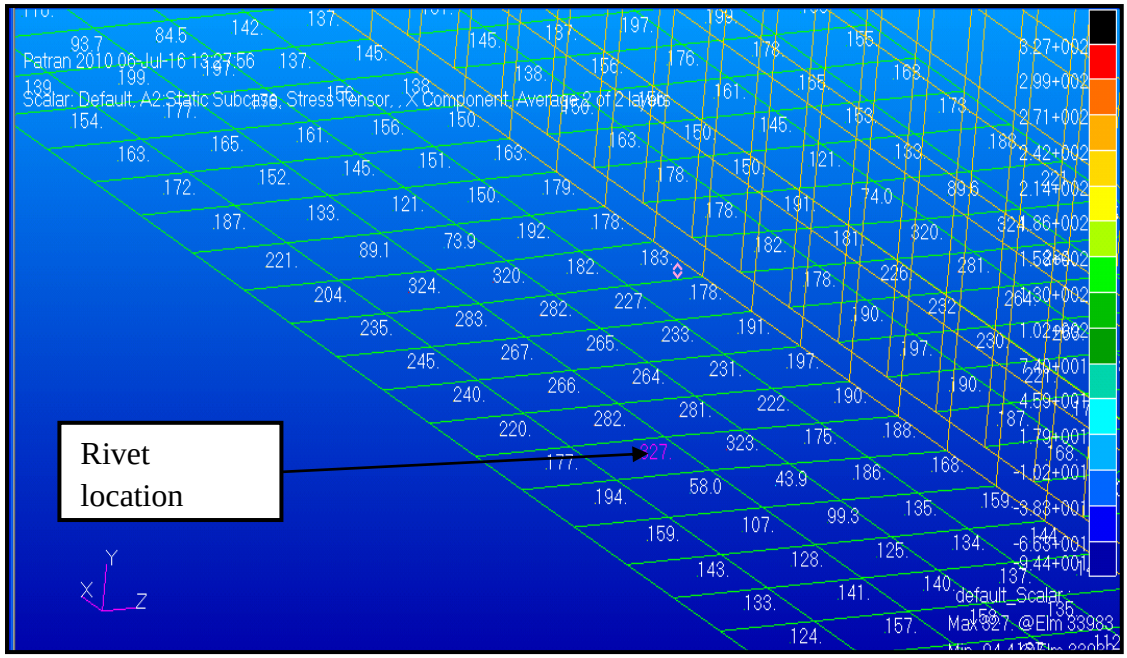

Figure 5.10 Maximum stress is obtained at 1 end of the rivet location.

The maximum stress is found at the one end of the rivet location, near to the bottom flange the obtained value is 327 N/mm^2 . However, the tensile yield strength of the aluminium 2024-T351 is 362 MPa. The induced stress level is found to be less than the allowable stress limit of the material used in the design of spar joint by using 2-D analysis. Hence, the static analysis of spar joint is considered to be safe design. Table 4.3 details the result summary of the static analysis of the spar joint using 2-D analysis.

CHAPTER 6

FATIGUE LIFE ESTIMATION

6.1 Introduction

Standard specimens tested under the constant amplitude loading have given a number of data on how materials behave under different fatigue conditions. However, during service period, structural components of aircrafts are subjected mostly to the variable amplitude loading. This implies that available fatigue data from tests under constant amplitudes cannot be applied without the appropriate modifications. Furthermore, the geometry of real component is very often significantly different from the geometry of the specimens, which could highly influence the accuracy of fatigue life predictions. In such a case, experimental verification of fatigue life of aircraft components under the variable amplitude loading must be carried out.

Normally aircraft wing will experience fluctuating loads during flight, due to this fluctuating loads crack initiate at critical region. Miners rule is adopted for the calculation of fatigue damage. The load factor G speaks to proportion of lift of an airplane to its weight.

6.2 MINER'S rule.

The easiest and most common practical method for estimating fatigue life estimation is the Palmgren – Miner speculation.

The hypothesis describes that fatigue damage at the given stress level is relative to the quantity of cycles at the applied stress level is partitioned by the aggregate number of cycles required to bring about disappointment at the same level.

Then the miner rule says that if the repeated loads are continued at the same level until the failure occurs, then the cycle ratio will be equal to.

From Miner's equation

$$\sum \frac{ni}{NF} = C \quad \ldots\ldots\ldots\ldots\ldots\ldots\ldots\ldots\ldots\ldots\ldots\ldots\ldots\ldots\ldots\ldots\ldots\ldots\ldots\ldots\ldots\ldots\ldots\ldots \ (4.2)$$

Were ni = applied number of cycles

N_f = number of cycles required to cause failure

The number of cycles to fracture (N_f) is found from the S-N curve for the material used. Figure 5.1 shows the S-N curve [2] of the material aluminum 2024-T351. In the graph stress range, mean stress and stress amplitude is drawn and the number of cycles to fracture is plotted between the mean stress and amplitude stress. The estimated load spectrum to which the aircraft subjected during its flight at high altitude is shown in table 5.1. The plot of maximum stress/minimum stress versus No of lift cycles is described bellow and the curve is known as S-N bend, as a rule the bend is plotted for the material Aluminum 2024 T351.

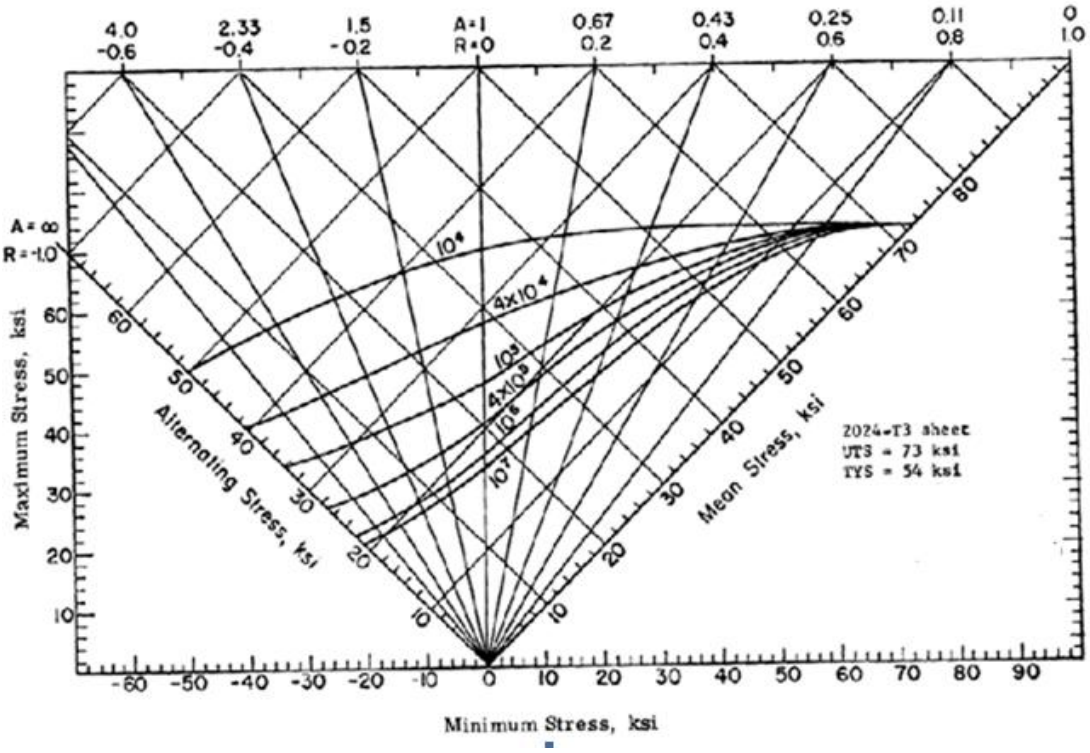

Figure 6.1 S-N curve for the aluminum 2024-T351

In this case the maximum stress is obtained at one end of the critical region in the bottom flange; the value is 327N/mm^2. Due to this stress concentration is created at the critical region due to this high tensile stress located at the flange, the fatigue crack is initiated.

Table 6.1 G condition with maximum stress

G condition	Maximum stress (N/mm^2)
1	4.147319
0.5	1.573659
0.75	2.359764
1	4.147319
1.25	4.933423
1.5	4.720978
1.75	5.507083
2	6.294638
2.5	7.868297
-0.5	4.147319

The following are the parameters that need to be considered in calculating the correction factor.

Stress concentration factor (SCF) = 1

Mean stress correction factor (MSCF) = 0.5

Design reliability (DR) = 0.897

Loading type (LT) = 1

Surface roughness (SR) = 0.8

6.3 Theoretical approaches to calculate damage accumulation

Correction factor can be determined by using the equation 5.2,

Correction factor= SCF × MSCF × DR × LT ×SR …… (5.2)

The mean stress can be calculated by using the equation 5.3

$$\sigma\text{mean} = \frac{(\sigma\text{max} + \sigma\text{min})}{2} \ldots\ldots\ldots\ldots\ldots\ldots\ldots\ldots\ldots\ldots\ldots\ldots\ldots\ldots..(5.3)$$

The mean stress with correction factor can be calculated by using the equation 5.3

$$\sigma\ \text{mean} = \frac{(\sigma\text{max} + \sigma\text{min})}{2\times\text{correction factor}} \ldots\ldots\ldots\ldots\ldots\ldots\ldots \ldots. \ldots (5.4)$$

The alternating stress can be calculated by using the equation 5.4

$$\sigma\text{alternating} = \frac{(\sigma\text{max} - \sigma\text{min})}{2}\ldots\ldots\ldots\ldots\ldots\ldots\ldots (5.5)$$

The range of stress is given by

$$R = \frac{\sigma\text{min}}{\sigma\text{max}} \ldots\ldots\ldots\ldots\ldots\ldots\ldots\ldots\ldots\ldots.. (5.6)$$

Damage accumulation can be determined by using,

$$D = \frac{Ni}{Nf}\ldots\ldots\ldots\ldots\ldots\ldots\ldots\ldots\ldots\ldots.. (5.7)$$

6.4: Determine the maximum stress of the wing spar of the wing spar joint

The maximum stress for different G condition was taken from the table 5.1. The number of Fatigue life cycle for different value of G condition is summarized in the table 5.2 was determined by using R, σ mean and σ alternating with correction factor from the S-N curve. Table 5.3 details the damage accumulation in Fatigue life cycle for different value of G using MINER’S rule.

Table 6.2 the number of Fatigue life cycle for different value of G condition

Range	Number of applied cycles (n_i)	σ_{max} (N/mm^2)	σ_{min} (N/mm^2)	Stress ratio (R)	Alternating stress N/mm^2
0.50g – 0.75g	40000	94.37527	64.23143	0.67	4.147319
0.75g – 1.10g	55000	62.28768	46.71576	0.75	1.573659
1.10g – 1.25g	38000	116.7535	94.40282	0.80	2.359764
1.25g – 1.50g	25000	184.1991	152.0552	0.00	4.147319
1.75g	500	38.92262	0	0.00	4.933423
2g	300	46.71576	0	0.00	4.720978
2.5g	250	54.49454	0	0.00	5.507083
-0.50g – 1.5 g	100	46.83284	-15.4548	-0.33	6.294638
-0.50g – 1.5g	50	57.24971	-20.6099	-0.36	7.868297

From the table 5.1 we confirmed that maximum stress is obtained at 2.5 G condition, the obtained value is 54.25Ksi and the minimum stress is obtained at -0.5 G condition, the obtained value is -10.85Ksi.

The alternating stress can be calculated as

$$б_a = \frac{бalt}{0.8*0.897} \ldots\ldots\ldots\ldots\ldots\ldots\ldots\ldots\ldots\ldots\ldots\ldots\ldots\ldots\ldots\ldots\ldots\ldots\ldots\ldots\ldots\ldots\ldots\ldots\ldots\ldots\ldots\ldots . (4.5)$$

The alternating stress and stress ratio are calculated for G condition as shown bellow

1. <u>For the range 0.5g – 0.75g</u>

Alternating stress

$$б_{alt} = \frac{\sigma max - \sigma min}{2} \ldots\ldots\ldots\ldots\ldots\ldots\ldots\ldots\ldots\ldots\ldots\ldots\ldots\ldots\ldots\ldots\ldots\ldots\ldots\ldots\ldots\ldots (4.6)$$

$б_{alt} = \frac{94.37527 - 64.23143}{2}$

$б_{alt}$ = 21.70Ksi

Stress ratio,

$$R = \frac{\sigma min}{\sigma max} \dots\dots\dots\dots\dots\dots\dots\dots\dots\dots\dots\dots\dots\dots\dots\dots\dots\dots\dots\dots\dots\dots\dots\dots\dots\dots\dots\dots\dots\dots . (4.7)$$

$$R = \frac{64.23143}{94.37527}$$

R = 0.67

2. <u>For the range 0.75g-1.10g</u>

Alternating stress

$$б_{alt} = \frac{\sigma max - \sigma min}{2}$$

$$б_{alt} = \frac{62.28768 - 46.71576}{2}$$

$б_{alt}$ = 10.85Ksi

Stress ratio,

$$R = \frac{\sigma min}{\sigma max}$$

$$R = \frac{64.23143}{94.37527}$$

R = 0.75

3. <u>For the range -0.50g – 1.5g</u>

$$б_{alt} = \frac{\sigma max - \sigma min}{2}$$

$$б_{alt} = \frac{57.24971 + 20.6099}{2}$$

$б_{alt}$ = 54.25

Stress ratio

$$R = \frac{\sigma min}{\sigma max}$$

$$R = \frac{20.6099}{57.2497}$$

R = -0.36

Table 5.3 damage accumulation in Fatigue life cycle for different value of G for using S-N curve

Range of G condition	Average G values	Applied no of cycles n_i	Number of cycles to failure N_f	Damage accumulated $\sum \frac{ni}{NF} = D_n$
0.50g – 0.75g	2.71	40000	Infinite	0
0.75g – 1.10g	2.71	55000	Infinite	0
1.10g – 1.25g	2.71	38000	Infinite	0
1.25g – 1.50g	2.71	25000	Infinite	0
1.75g	18.99	500	$6*10^5$	$8.33*10^4$
2g	21.70	300	$2*10^5$	$1.50*10^4$
2.5g	27.12	250	$5*10^5$	$5.00*10^4$
-0.50g – 1.5 g	21.70	100	$4*10^5$	$2.50*10^4$

1. The damage accumulated for the range 0.50g-0.75g is given as

Damage accumulated

$$\sum \frac{ni}{NF} = D_n$$

$$= \frac{40000}{Infinite}$$

$$= 0$$

2. For the range 1.75g

$$= \sum \frac{ni}{NF} = D_n$$

$= \frac{40000}{\text{Infinite}}$

$= 8.33*10^4$

Summation of damage accumulation

D a = D1 + D2 + D3 + D4 + D5 + D6 + D7 + D8………………………….…… (4.8)

D a = 0 + 0 + 0 + 0 + $8.33*10^4 + 1.50*10^4 + 5.00*10^4 + 2.50*10^4$

D a = $7.583 *10^{-3}$

The damage accumulation was found to be less than one ($7.583*10^{-3}$). Hence, it can be concluded that the crack would not initiate in the critical region obtained at the one part of the rivet location.

Hence further the total damage accumulated is 7.583*10-3 for 1 block which is required to cause for 10 flying hours which means for 1 flight, for 100 flight which is required for 100 flying hours, hence the total damage flying hours is calculated as shown bellow

$$\text{Total damage flying hours} = \frac{1}{\text{total damage accumulated}} \ldots\ldots\ldots\ldots\ldots\ldots\ldots\ldots (4.9$$

$= \frac{1}{7.583*10-3}$

= 1.31873*10-4

Hence the total damage flying hours is 1.31873*10-4 is required to cause fatigue damage so further maintenance is required for the critical region in the damaged structure with in this flying hours.

CHAPTER 7

CONCLUSIONS

In the present work, the finite element analysis is carried out on the wing spar joint by considering light jet aircraft structure, using MSC NASTRAN/PATRAN software. From the Static analysis, it is found that for the 1-D analysis the maximum stress obtained is 350 N/mm^2, which is well within the allowable stress of the material so an obtained design is considered to be safest design. From the Static analysis, it is found that for the 2-D analysis maximum stress obtained is 346 N/mm^2, which is well within the allowable stress of the material so an obtained design is considered to be safest design. From the Static analysis, it is found that the maximum stress obtained at one end of the rivet location is 327 N/mm^2, so the maximum stress obtained is not exactly the allowable stress of the material so obtained design is considered to be safest design.

In phase 2 the damage accumulated is safest design that is maximum stress obtained at one part of the rivet location is calculated. From miner's rule it has been proved that the damage accumulation value is less than one, so concluded that for considered load spectrum crack would not initiate in the structure.

In future the fatigue life estimation can be completed on the other parts of the wing structure. In further the essential lug joint can be included for the wing fight joint rather than C clamp by remembering the idea of weight optimization. In future studies instead of C clamp joint, the lug joint can be placed between the spars and the analysis can be carried out.

REFERENCES

1. Aleksandar grbovic and Bosko rasuo, “FEM based exhaustion break development forecasts for fight of lightaircraft under variable plentifulness stacking”, 1st International Conference on Structural Integrity, ICONS-2014
2. Nagarjun C M, Nagaraj V C, Byrareddy and K E Girish, “Stress Examination of Flat Tail Joint of a Vehicle Air ship and Fatigue Life Estimation”, IJSRD - International Journal for Scientific Research & Development| Vol. 3, Issue 04, 2015 | ISSN (online): 2321-0613
3. Rhys Jones, Daren Peng, Pu Huang, Raman R. K. Singh, “Break development from normally happening material discontinuities in operational air ship”, 3rd international conference on material and component performance under variable amplitude loading, VAL 2015.
4. R.M. Ajaj , M.I. Friswell , M. Bourchak , W. Harasani, “Range transforming utilizing the GNATSpar wing”, aeronautics and astronautics, university of Southampton, S0171BJ,UK.
5. Harish E.R.M1, Mahesha.K2, Sartaj Patel3, “ stress analysis of an wing attachment bracket for an transport aircraft structure”, Vol. 2, Issue 7, July 2013
6. Raffaele Sepe, Enrico Armentani and Francesco Caputo, “static and fatigue experiments of an full scale fuselage panel and fatigue analysis”, R. Sepe et alii, Frattura ed Integrità Strutturale, 35 (2015) 534-550; DOI: 10.3221/IGF-ESIS.35.59
7. Polagnagu James*, Kotresh Gaddikeri , Byji Varughese and M. Subba Rao, "realization of an ideal wing test structure of an idelaised wing box”, 1st International Conference on Structural Integrity, ICONS-2014
8. Ralph l stephens , Ali fatemi , Robert r stephens , Henry o fuchs, “metal weariness in designing”,
9. Mohamed Hamdan A1, Nithiyakalyani S2, “ design and analysis of an wing and spar of the swept back wing”, (ISSN 2250-2459, ISO 9001:2008 Certified Journal, Volume 4, Issue 12, December 2014)

APPENDIX

PATRAN is one type of internal programming language (PCL). It is used to build geometry and to define mesh and allow finite element analysis using MSC NASTRAN.

MODEL 1: Design of 1D wing spar joint of a transport aircraft structure for static analysis.

Step 1- creating data base

Launch -> File -> new, name your first .db – ok- default under tolerance-structural analysis type -> apply

Step 2- creating group

Create separate group for geometry, 2D element and 1D element.

Group -> create group name – apply-> type another group name if required apply

Set current to the particular group

Group-> set current group name -> apply

Post option is to post the particular group

Group -> set current group-> apply

Step 3- creating geometry

Geometry-> create – point –method- points coordinate list-> apply

Geometry-> create – curve- method – option – starting point list- ending point list -> apply

Figure shows the geometry of the model after completing the above steps

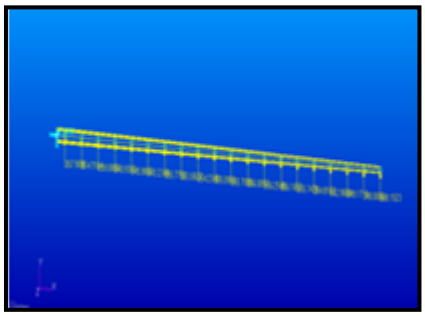

Figure A1: Geometric model for 1D analysis

Step 4- Finite element model

Elements->create - mesh-curve- topology- select curve list-value -automatic calculation -> apply

Step 5- load and boundary conditions

The bellow steps shows the creating boundary conditions

Load and boundary conditions-> create – displacement – type – nodal – new set name- input data – set application region - apply

Load and boundary conditions-> create – force – type – nodal – new set name – input data – set application region - apply

Figure shows the load and boundary conditions used in 1D analysis

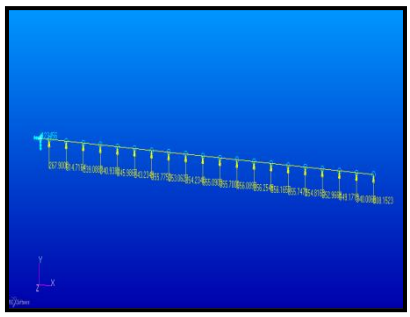

Figure A2 Load and boundary conditions used in 1D analysis

Step 6- material

Material-Create – isotropic –method – material name – input properties - apply

Under input properties the modulus of elasticity and poisons ratio is selected

Step 7- properties

Properties – create – type – object-new set name – general section- input properties

Under input properties the material name, bar orientation, new section name is selected- set application region-ok – apply

Step 8 - analysis

Analysis – analysis – entire model – analysis deck- sub cases select- select all – apply

Step 9 – run the analysis in MSC software

Open the software – select the result file folder – type SCR=Y- apply

Step 10- results

Results – create – quick plot – beam stresses maximum combined – displacement translational -apply

Figure A3 shows the Static analyses of spar joint by using 1D. Figure A4 shows the Deformation of spar joint by using 1D analysis.

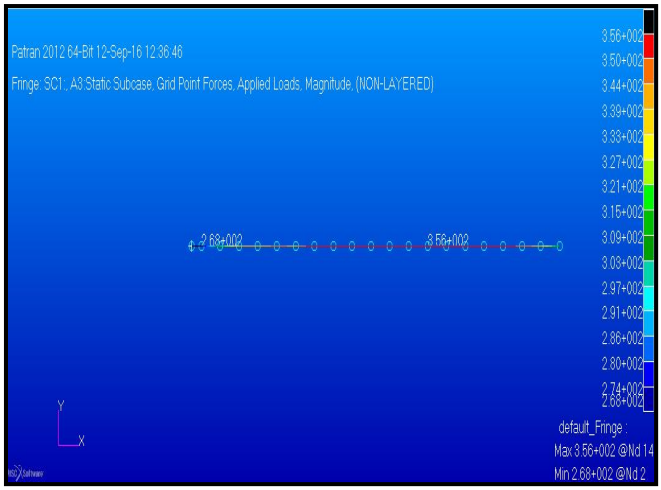

Figure A3 Static analyses of spar joint by using 1D

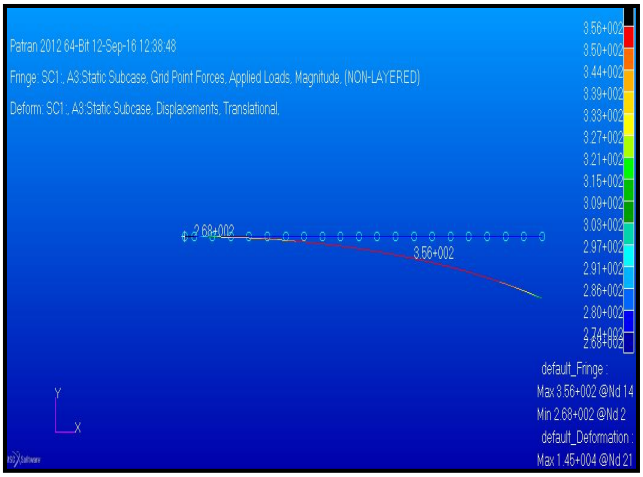

Figure A4 Deformation of spar joint by using 1D analysis.

Step 11 – plotting bending moment

Results – create – report – overwrite file – beam force rotation (bending moment) – target entities – change to nodes – select all – displacement attribute- file – name – ok- plot options – go to global - apply

Figure A5 shows the maximum bending moment analysis in 1D

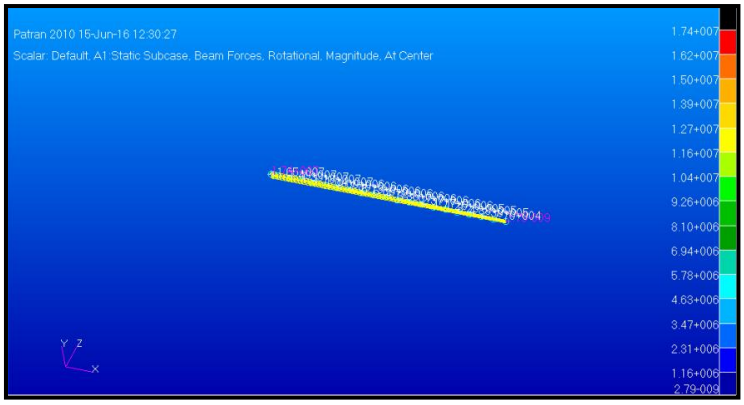

Figure A5 Maximum bending moment analysis in 1D

Generate bending moment file from software to excel sheet

MS excel -> open – all files – bending moment – yes – delimited – next- semi colon – space – next - finish

MODEL 2: 2D wing spar joint of a transport aircraft structure for static analysis

Step 1- creating data base

Launch -> File -> new, name your first .db – ok- default under tolerance-structural analysis type -> apply

Step 2- creating group

Create separate group for geometry, 2D element and 1D element.

Group -> create group name – apply-> type another group name if required apply

Set current to the particular group

Group-> set current group name -> apply

Post option is to post the particular group

Group -> set current group-> apply

Step 3- creating geometry

Geometry-> create – point –method- points coordinate list-> apply

Geometry-> create – curve- method – option – starting point list- ending point list -> apply

Figure shows the geometry of the model after completing the above steps

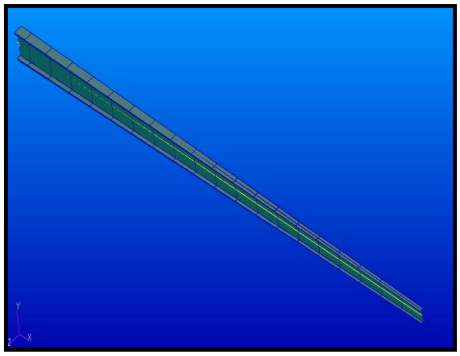

Figure A6 Geometric model for 2D analysis

Step 4- Finite element model

Elements->create - mesh- 2curves - topology- select curve 1 and curve 2 list-value - automatic calculation -> apply

To check the verification of quad element

Equivalence – all – tolerance cube – set tolerance to 0.005 – verify – reset - apply

To check the aspect ratio

Verify – quad – apply

Figure A7 shows the finite element model used in 2D analysis

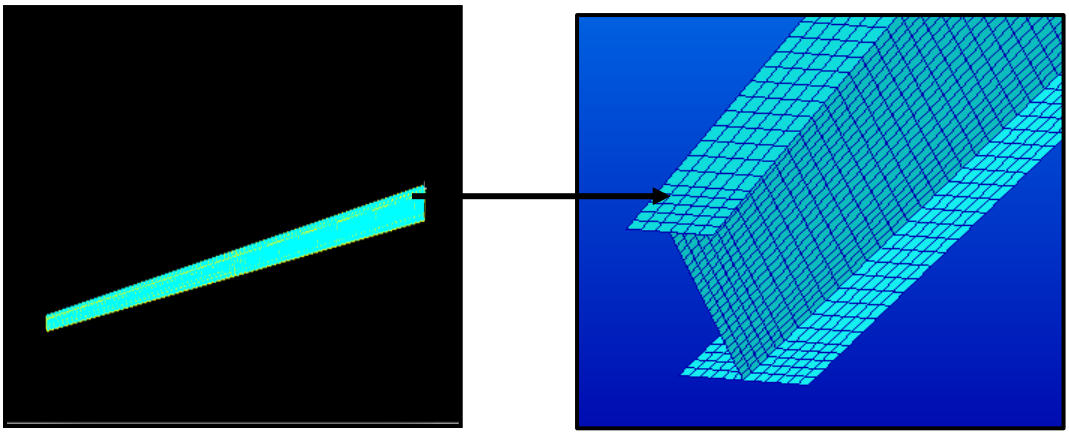

Figure A7: Finite element model of spar joint

Step 5- load and boundary conditions

The bellow steps shows the creating boundary conditions

Load and boundary conditions-> create – displacement – type – nodal – new set name- input data – set application region - apply

Load and boundary conditions-> create – force – type – nodal – new set name – input data – set application region - apply

Figure A8 shows the load and boundary conditions used in 2D analysis

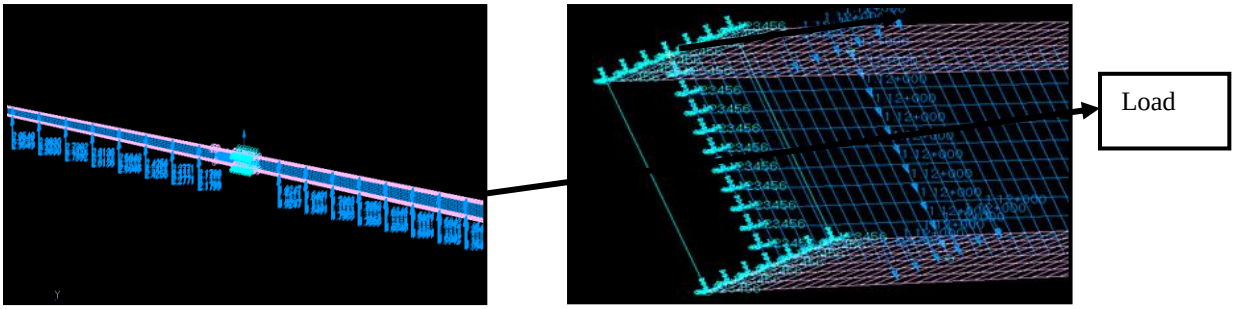

Figure A8: Load and boundary conditions of the spar joint

Step 6- material

Material-Create – isotropic –method – material name – input properties - apply

Under input properties the modulus of elasticity and poisons ratio is selected

Step 7- properties

Properties – create – type – object-new set name – general section- input properties

Under input properties the material name, bar orientation, new section name is selected- set application region-ok – apply

Step 8 - analysis

Analysis – analysis – entire model – analysis deck- sub cases select- select all – apply

Step 9 – run the analysis in MSC software

Open the software – select the result file folder – type SCR=Y- apply

Step 10- results

Results – create – quick plot – stress tensor – displacement translational -apply

Figure A9 shows the Static analyses of spar joint by using 1D. Figure A10 shows the Deformation of spar joint by using 2D analysis.

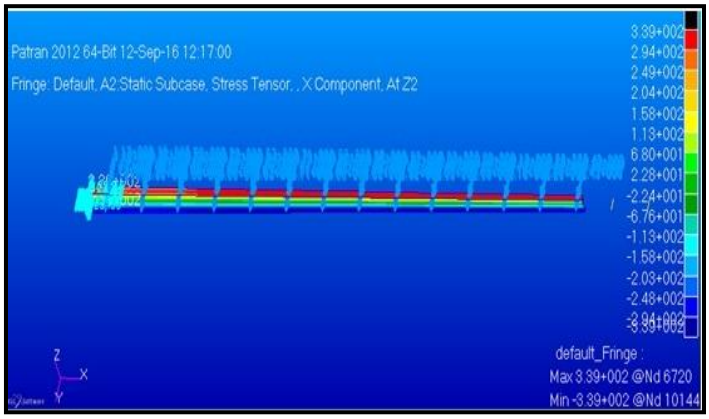

Figure A9 Static analysis of spar beam using 2-D

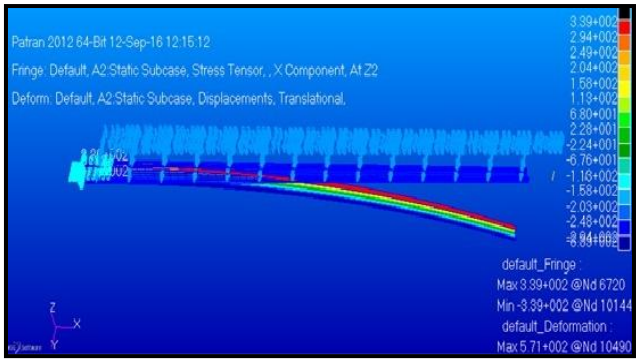

Figure A10 Deformation of spar beam by using 2D analysis

MODEL 3: Determine the maximum stress on the wing spar joint and to maintain within the yield criteria.

Step 1- creating data base

Launch -> File -> new, name your first .db – ok- default under tolerance-structural analysis type -> apply

Step 2- creating group

Create separate group for geometry, 2D element and 1D element.

Group -> create group name – apply-> type another group name if required apply

Set current to the particular group

Group-> set current group name -> apply

Post option is to post the particular group

Group -> set current group-> apply

Step 3- creating geometry

Geometry-> create – point –method- points coordinate list-> apply

Geometry-> create – curve- method – option – starting point list- ending point list -> apply

Figure shows the geometry of the model after completing the above steps

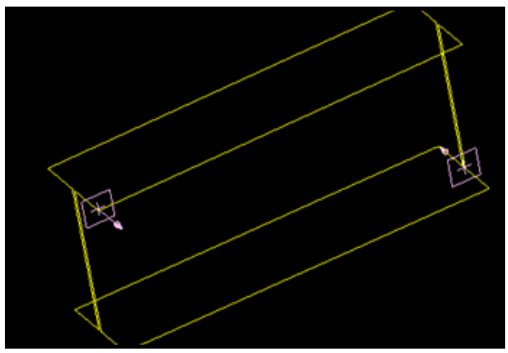

Figure A11 Geometric configuration of C clamp joint

Step 4- Finite element model

Elements->create - mesh- 2curves - topology- select curve 1 and curve 2 list-value - automatic calculation -> apply

To check the verification of quad element

Equivalence – all – tolerance cube – set tolerance to 0.005 – verify – reset - apply

To check the aspect ratio

Verify – quad – apply

Figure A12 shows the finite element model used in 2D analysis

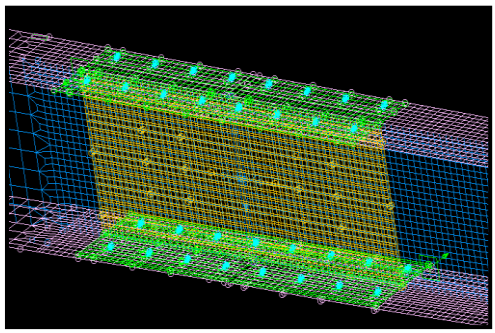

Figure A12 Finite element model of spar joint

Step 5- load and boundary conditions

The bellow steps shows the creating boundary conditions

Load and boundary conditions-> create – displacement – type – nodal – new set name- input data – set application region - apply

Load and boundary conditions-> create – force – type – nodal – new set name – input data – set application region - apply

Figure A13 shows the load and boundary conditions used in 2D analysis

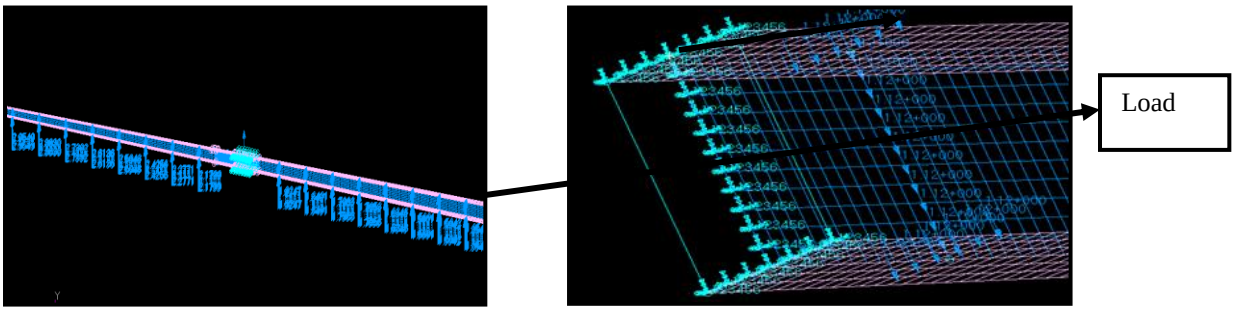

Figure A13: Load and boundary conditions of the spar joint

Step 6 – designing of rivets

Properties – create – 1D – beam – property set name – input properties – set material name – bar orientation – cross section name – new section name-radius- ok - apply

Select application region – entities – members – ok - apply

Figure A14 shows the finite element model of rivet in 3D

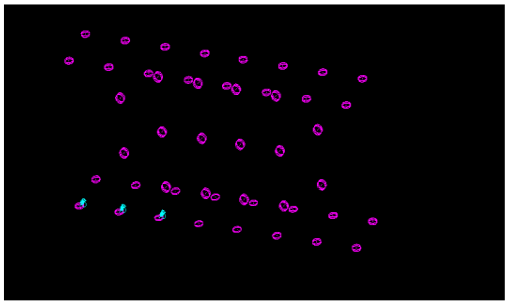

Figure A14 Finite element model of rivet in 3D

Step 6- material

Material-Create – isotropic –method – material name – input properties - apply

Under input properties the modulus of elasticity and poisons ratio is selected

Step 7- properties

Properties – create – type – object-new set name – general section- input properties

Under input properties the material name, bar orientation, new section name is selected- set application region-ok – apply

Step 8 - analysis

Analysis – analysis – entire model – analysis deck- sub cases select- select all – apply

Step 9 – run the analysis in MSC software

Open the software – select the result file folder – type SCR=Y- apply

Step 10- results

Results – create – quick plot – stress tensor – displacement translational -apply

Figure A15 shows the Static analyses of spar joint by using 1D. Figure A16 shows the Deformation of spar joint by using 2D analysis.

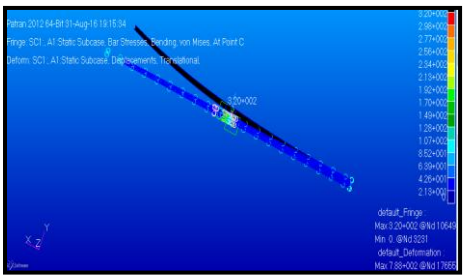

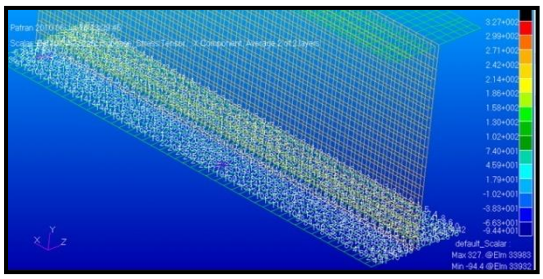

Figure A15 Deformation of 2-D spar joint Figure A16 Shows the Static analyses of spar joint